One mucosal administration of a live attenuated recombinant COVID-19 vaccine protects non-human primates from SARS-CoV-2

Mariana F. Tioni[1,8], Robert Jordan[1,4,8], Angie Silva Pena[1], Aditya Garg[1], Danlu Wu[1], Shannon I. Phan[1], Xing Cheng[1], Jack Greenhouse[2], Tatyana Orekov[2], Daniel Valentin[2], Swagata Kar[2], Laurent Pessaint[2], Hanne Andersen[2], Christopher C. Stobart[5], Melissa H. Bloodworth[6], R. Stokes Peebles Jr.[6,7], Yang Liu[3], Xuping Xie[3], Pei-Yong Shi[3], Martin L. Moore[1], Roderick S. Tang[1]

[1]Meissa Vaccines Inc, Redwood City, CA 94065

[2]BIOQUAL Inc., Rockville, MD 20850

[3]Department of Biochemistry and Molecular Biology, University of Texas Medical Branch, Galveston TX 77550

[4]Present address: Bill & Melinda Gates Foundation, Seattle WA 98102

[5]Department of Biological Sciences, Butler University, Indianapolis, IN 46208

[6]Division of Allergy, Pulmonary and Critical Care Medicine, Department of Medicine, Vanderbilt University School of Medicine, Nashville, TN 37232

[7]Department of Pathology, Microbiology, and Immunology, Vanderbilt University School of Medicine, Nashville, TN 37232

[8]Joint first authors

Corresponding author: Mariana Tioni, Meissa Vaccines Inc, 1100 Island Drive, Suite 202, Redwood City, CA 94065. mariana.tioni@meissavaccines.com

Acknowledgement

We thank Anthony Cook, Renita Brown, Tammy Putmon-Taylor, Tracey-Ann Campbell, Shanai Browne, Zack Flinchbaugh, Elyse Teow and Jason Velasco at Bioqual for animal care support and technical expertise with our African green monkey study. We thank Douglas Haney for biostatistics support and Nexelis for sharing pseudovirus neutralization assay and reagents. We thank Tina V. Hartert from the Peebles' lab for the TN 12/11-19 RSV strain and hVIVO for the Memphis 37b RSV strain. We are grateful to Janelle Muranaka for technical and logistical support.

Abstract

Severe Acute Respiratory Syndrome Coronavirus 2 (SARS-CoV-2) is the causative agent of the COVID-19 global pandemic. Vaccines are needed to control the disease and bring an end to the pandemic. SARS-CoV-2 is an enveloped RNA virus that relies on its trimeric surface glycoprotein, spike, for entry into host cells. Here we describe the COVID-19 vaccine candidate MV-014-212, a live attenuated, recombinant human respiratory syncytial virus (RSV) expressing a chimeric SARS-CoV-2 spike as the only viral envelope protein. MV-014-212 was attenuated and immunogenic in African green monkeys (AGMs). One mucosal administration of MV-014-212 in AGMs protected against SARS-CoV-2 challenge, reducing the peak shedding of SARS-CoV-2 in the nose by more than 200-fold. MV-014-212 elicited mucosal immunity in the nose and neutralizing antibodies in serum that exhibited cross neutralization against two virus variants of concern. Intranasally delivered, live attenuated vaccines such as MV-014-212 entail low-cost manufacturing suitable for global deployment. MV-014-212 is currently in phase I clinical trials as a single-dose intranasal COVID-19 vaccine.

Introduction

COronaVIrus Disease 2019 (COVID-19) is the latest virus pandemic to afflict humanity. The spread of the disease started in the late months of 2019 (Zhou 2020, Wu 2020), and by March 11th of 2020 118,000 people in 114 countries were infected at which time it was declared a pandemic by the World Health Organization (WHO) (WHO, March 2020). COVID-19 is a respiratory disease often leading to pneumonia caused by the highly transmissible Severe Acute Respiratory Syndrome Coronavirus 2 (SARS-CoV-2, *Coronaviridae* Study Group of the International Committee on Taxonomy of Viruses 2020). It has an overall mortality rate of approximately 2% and is especially severe in the elderly and patients with serious underlying medical conditions, such as heart or lung disease and diabetes. As of 5th July 2021, there were 183,560,151 confirmed cases of SARS-CoV-2 infection with a total of 3,978,581 deaths worldwide (WHO dashboard, https://covid19.who.int/).

SARS-CoV-2 is an enveloped RNA virus that relies on its surface glycoprotein, spike, for entry into host cells (Letko 2020, Shang 2020). The spike protein is a type I fusion protein that forms a trimer which protrudes on the viral membrane giving the virus its characteristic appearance of a crown under electron microscopy (Turoňová 2020, Li 2015). The angiotensin converting enzyme 2 (ACE2) has been identified as a cellular receptor for SARS-CoV-2 spike (Letko 2020, Hoffmann, Cell 2020). Disrupting the interaction of ACE2 and the receptor binding domain (RBD) of spike is at the core of vaccine design and therapeutics. Currently, three COVID-19 vaccines have been approved for emergency use in the US (CDC, "Authorized and Recommended Vaccines"). The three vaccines are based on SARS-CoV-2 spike protein, and their high level of efficacy has validated spike as a protective antigen.

All the EUA vaccines currently in use are delivered intramuscularly, and none of them is live attenuated. Live attenuated vaccines (LAVs) are often administered by the same route of entry as the pathogen they target, and LAVs replicate in the host, mimicking natural infection without causing disease. For respiratory viruses, intranasal LAVs generate mucosal immunity at the site of infection, blocking the pathogen at the earliest phases of infection thus helping control systemic spread (Holmgren 2005). In the case of influenza infection, LAV induces better mucosal IgA and cell-mediated immunity relative to other vaccine types, eliciting a longer lasting and broader immune response that more closely resembles natural immunity (Cox 2004). Furthermore, comparison of intramuscularly and intranasally administered vaccines against SARS-CoV in mice showed that serum IgA was only induced following intranasal vaccination (See 2006), and only intranasal vaccination provided protection in both upper and lower respiratory tract (Hassan 2020). For SARS-CoV-2 in particular, the early antibody response is dominated by IgA and mucosal IgA is highly neutralizing (Sterlin 2021), underscoring the importance of developing an intranasal vaccine capable of eliciting mucosal immunity. According to the WHO vaccine tracker, there are currently 105 vaccines in clinical trials, only 3 of which are intranasal replicating vaccines (WHO, **Draft landscape and tracker of COVID-19 candidate vaccines**).

Here we describe the rational design, generation, and pre-clinical evaluation of a novel COVID-19 vaccine candidate. MV-014-212 is a live attenuated recombinant vaccine strain derived from the human respiratory syncytial virus (RSV) vaccine candidate OE4 (Stobart, 2016). In MV-014-212, the RSV attachment (G) and fusion (F) surface glycoproteins were replaced with a chimeric SARS-CoV-2 spike harboring the cytoplasmic tail of the RSV F protein. MV-014-212 was attenuated and immunogenic in non-human primates producing both systemic and mucosal immunity after one mucosal administration. A single mucosal administration of MV-014-212 in African green monkeys (AGMs) elicited neutralizing antibodies against the homologous virus and cross neutralizing activity against the variants of concern B.1.351 and B.1.1.7. Studies in mice indicated that MV-014-212 vaccination generated a Th1-biased cellular immune response. MV-014-212 is currently being evaluated in phase I clinical trials as a single-dose intranasal COVID-19 vaccine.

Results

Design and Generation of MV-014-212

MV-014-212 is a novel live attenuated, recombinant vaccine against SARS-CoV-2, based on the backbone of the human respiratory syncytial virus (RSV) (Fig. 1). The G and F proteins of RSV were replaced by a chimeric protein consisting of the ectodomain and transmembrane (TM) domains of SARS-CoV-2 spike (USA-WA1/2020) and the cytoplasmic tail of RSV F (strain line19). The rational design of this chimera was based on previous observations of the need for the homologous TM of spike in coronavirus infectious particle production (Godeke 2000, Broer 2006, Corver 2009) and the reported importance of the cytoplasmic tail of RSV F in the production of RSV progeny (Oomens 2006). The sequence of amino acids at the junction between spike and F proteins is shown in Fig. 1. Notably, the chimeric spike/RSV F protein retains functionality as MV-014-212 growth relies on it for attachment and fusion with the host cell. Various chimeric spike constructs that differed in the junction position were assessed for growth in Vero cells (Fig. S1). In particular, a construct with the entire native SARS-CoV-2 spike was evaluated (MV-014-300, Fig. S1). While this construct could be rescued, it did not propagate productively in cell culture, demonstrating that the cytoplasmic tail of the F protein contributes to viral growth of the chimeric virus expressing spike. Of the constructs expressing different chimeric spike/RSV F fusion proteins, MV-014-212 was selected for further evaluation based on the ease of rescue and its ability to grow to acceptable titers for pre-clinical and clinical studies.

The RSV backbone used to generate MV-014-212 was attenuated for replication in primary cells by codon deoptimization of the genes encoding the proteins NS1 and NS2 that suppress host innate immunity (Meng 2014). In addition, the short hydrophobic glycoprotein SH was deleted (Fig. 1) to further attenuate the virus *in vivo* and increase transcription of downstream genes (Stobart 2016).

To facilitate the development of a microneutralization assay, a reporter virus derived from MV-014-212 was constructed by inserting the gene encoding the fluorescent mKate2 protein (Hotard 2012, Shchervo 2009) upstream of the NS1 gene (MVK-014-212, Fig. 1).

The recombinant virus constructs were electroporated into Vero cells and infectious virus was rescued and propagated for further characterization using an approach described previously (Hotard 2012). In MV-014-212, CPE is observed as the formation of polynucleated bodies or syncytia and eventual cell detachment (Fig. 2A). The electroporated cells were expanded until the CPE was extensive and the virus stock was harvested as a total cell lysate. The titers obtained for MV-014-212 and MVK-014-212 were comparable and within the range $1\text{-}5\times10^5$ PFU/mL.

In vitro Characterization of MV-014-212

The SARS-CoV-2 spike protein contains a cleavage site between the S1 and S2 domains that is processed by furin-like proteases (Fig. 1 and Hoffmann 2020). As for other coronaviruses, the S1 and S2 subunits of SARS-CoV-2 spike are believed to remain non-covalently bound in the prefusion conformation after cleavage (Walls 2020, Burkard 2014). To determine if the chimeric spike protein encoded by MV-014-212 is expressed and proteolytically processed, virus stocks prepared from lysates of infected Vero cells were analyzed on western blots and probed with polyclonal antiserum against SARS-CoV-2 spike protein. Both MV-014-212 and MVK-014-212 viruses express the full length and cleaved forms of the chimeric spike protein (Fig. 2B), consistent with partial cleavage at the S1-S2 junction, with the expected apparent sizes (Fig. S2, Ou 2020, Peacock 2021).

Multi-cycle growth kinetics of MV-014-212 was compared to wild type recombinant RSV A2 in Vero cells (Fig. 2C). MV-014-212 exhibited delayed growth kinetics relative to RSV A2 showing an initial lag phase of approximately 12 hours. Both viruses reached their peak titers at 72 hpi and the titers remained constant until 120 hpi. The peak titer for MV-014-212 was approximately one order of magnitude lower than that of RSV A2. To determine if the insertion of the mKate2 gene affected replication kinetics of MVK-014-212, Vero cells were infected with MV-014-212 or MVK-014-212. The growth kinetics of MVK-014-212 was similar to that of MV-014-212 reaching comparable peak titers by 72 hpi (Fig 2D). These data are consistent with a report that insertion of mKate2 in the first gene position did not significantly attenuate RSV A2-line19F *in vitro* (Hotard 2012).

To evaluate the short-term thermal stability of MV-014-212, aliquots of the viral stock were incubated at different temperatures for a period of 6 hours and the amount of infectious virus after the incubation was determined by plaque assay. Two stocks of MV-014-212 prepared in different excipients were compared in this study (Fig 2E). The results demonstrate that MV-014-212 is stable for at least 6 hours in either excipient at -80°C and room temperature.

The genetic stability of MV-014-212 was examined by serial passaging in Vero cells. Subconfluent Vero cells were infected in triplicate with an aliquot of MV-014-212 and passaged for 10 consecutive passages (Fig. S3). Viral RNA was isolated from passages 0 and 10 and amplified by RT-PCR. The sequence of the entire coding regions of the viral genome was determined by Sanger sequencing. The results showed for all three lineages there were no variations detected at passage 10 relative to the starting stock (passage 0). Thus, the vaccine candidate was highly genetically stable *in vitro*.

MV-014-212 replication is attenuated in African green monkeys and confers protection against *wt* SARS-CoV-2 challenge

African green monkeys (AGMs) are semi-permissive for replication of both *wt* SARS-CoV-2 (Woolsey 2021, Cross 2020, Blair 2021, Lee 2021) and RSV (Taylor 2017) and therefore constitute an appropriate non-human primate model for studying the attenuation and protective immunity of MV-014-212.

The AGM study design is depicted in Fig. 3A. On Day 0, AGMs were inoculated via the intranasal (IN) and intratracheal (IT) routes with 1.0 mL of 3×10^5 PFU/mL MV-014-212 or *wt* RSV A2 at each site for a total dose of 6×10^5 PFU per animal. Due to the semi-permissive nature of the AGM model, intratracheal inoculation was necessary to promote replication of the vaccine and the SARS-CoV-2 challenge virus in the lungs. Animals in the mock group were similarly mock inoculated with PBS. Nasal swabs (NS) and bronchoalveolar lavage (BAL) samples were collected through day 12 after immunization. Viral shedding in NS and BAL samples was determined by plaque assay using fresh samples that were not frozen at the study site. The results showed that the level of infectious virus in animals inoculated with MV-014-212 and duration of shedding in nasal secretions was lower than animals inoculated with RSV A2 (Fig. 3B and S4). The mean peak titer for RSV A2 was approximately 20-fold higher than that observed for MV-014-212 inoculated animals. These results show that MV-014-212 is attenuated in the upper respiratory tract of AGMs compared to RSV A2.

Low to undetectable virus titers were also observed in the lower respiratory tract of animals inoculated with MV-014-212 or RSV A2 over the course of 12 days. Both viruses replicated at low levels, but peak levels occurred earlier for MV-014-212. In this study, RSV A2 showed 100- to 1,000-fold lower peak titers in the lower respiratory tract of AGMs compared to wild-type RSV A2 titers reported in literature (Cheng 2001, Jin 2003, Tang 2004, Nouen 2014), confounding the ability to assess attenuation of MV-014-212 in the lungs. Subsequently, lower titers were also observed in the lungs of cotton rats for the recombinant A2 used in this study (rA2 from Meissa Vaccines Inc., Fig. S5), relative to biologically derived RSV strains suggesting that the RSV A2 used in this AGM study was attenuated in lungs.

Nasal and BAL samples from day 6 post vaccination were used to extract RNA for sequence analyses of the spike gene of MV-014-212. Using Sanger sequencing, no variations in the spike gene were detected compared to the reference sequence for MV-014-212.

On day 28 AGMs were challenged with 10^6 $TCID_{50}$ of *wt* SARS-CoV-2. NS and BAL samples were collected for 10 days after challenge. Shedding of wt SARS-CoV-2 was measured by RT-qPCR of the E gene sub-genomic SARS-CoV-2 RNA (sgRNA) (Fig. 3C and S6).

MV-014-212 vaccinated monkeys had low or undetectable levels of *wt* SARS-CoV-2 sgRNA in NS samples in contrast to animals inoculated with *wt* RSV A2 or PBS (mock) which had higher levels of SARS-CoV-2 sgRNA. While the level of SARS-CoV-2 sgRNA was undetectable in animals vaccinated with MV-014-212 at most time points, one animal had detectable SARS-CoV-2 sgRNA at day 2 and a different animal had a similar titer at day 4 post-challenge (Fig. S6). Mean peak titers of SARS-CoV-2 in NS of animals in the control RSV and PBS groups were 20 and 250-fold higher than for animals vaccinated with MV-014-212, respectively. In both RSV and mock infected animals, shedding of *wt* SARS-CoV-2 sgRNA decreased steadily in nasal secretions from day 4 to 10, and by day 10 all animals in both groups had undetectable SARS-CoV-2 sgRNA.

Vaccination with MV-014-212 resulted in increased clearance of SARS-CoV-2 in lungs compared to animals inoculated with RSV A2 or mock-inoculated with PBS (Fig. 3C and S6). The peak titer of SARS-CoV-2 in BAL samples occurred at Day 2 and was similar in all three treatment groups. Lung titers were undetectable in MV-014-212 vaccinated animals on Day 4 through day 10 while SARS-CoV-2 was readily measured in animals inoculated with RSV A2 or mock-vaccinated. Shedding of infectious SARS-CoV-2 in BAL and NS after challenge was quantified by a TCID50 assay (Fig. S7). The results show that AGMs vaccinated with MV-014-212 had on average between 100 and 1000-fold less infectious SARS-CoV-2 in BAL than the RSV A2 and mock controls at peak shedding days. The kinetic of clearance of the MV-014-212 group was also faster, in accordance with the results obtained by sgRNA qPCR assay. In NS, the average peak shedding of the vaccinated group was more than 1000-fold lower than that of the RSV A2 group (Fig. S7). In the NS of the mock-vaccinated group, however, one of the animals did not have detectable shedding of infectious virus at any of the time points (Fig. S7). As a result, the overall average peak shedding was only 30-fold higher than that of the MV-014-212 vaccinated group.

Taken together, these data show that a single mucosal administration of MV-014-212 protected AGMs from *wt* SARS-CoV-2 challenge.

Antibody responses to MV-014-212 vaccination in AGMs

SARS-CoV-2 spike-specific serum IgG and nasal IgA were measured by ELISA in sera and nasal swabs, respectively, from AGMs immunized with MV-014-212, RSV A2, or PBS on Day 25 post-

immunization. All animals were seronegative for RSV A2 and SARS-CoV-2 at the start of the study. AGMs inoculated with MV-014-212 produced higher levels of SARS-CoV-2 spike-specific IgG in serum compared to AGMs inoculated with RSV A2 or PBS, which had levels of spike-specific IgG that were close to the limit of detection (Fig. 4A).

Spike-specific IgA was also detected in the nasal swabs of monkeys inoculated with MV-014-212. There was more than an 8-fold increase in nasal spike-specific IgA in the MV-014-212 vaccinated animals 25 days after vaccination (Fig. 4B). In contrast, RSV A2 or mock vaccinated animals did not show a significant change in spike-specific IgA.

These results showed that mucosal inoculation of MV-014-212 induced both nasal and systemic antibody responses to the functional SARS-CoV-2 spike.

To determine if vaccination with MV-014-212 elicited neutralizing antibodies in AGMs, three different approaches were used: (a) microneutralization assays with a fluorescent reporter homologous virus (MVK-014-212), (b) vesicular stomatitis virus (VSV) pseudovirus neutralization assays and (c) plaque reduction assay with SARS-CoV-2 viruses. Fig. 5A shows a representative microneutralization assay where the fluorescent reporter MVK-014-212 was used to infect Vero cells in a 96-well plate. This assay was used to quantify the neutralizing titers (NT50) of AGMs vaccinated with MV-014-212 or the control groups inoculated with RSV or mock-inoculated (Fig. 5B). The AGMs vaccinated with MV-014-212 showed an average NT50 of 99 whereas the RSV A2 and mock controls had an NT50 of 16 and 14, respectively. The same sera were used in a pseudovirus neutralization assay based on spike-pseudotyped VSV particles carrying the luciferase reporter gene (Fig. S8). The results of the VSV pseudovirion assay showed a similar trend but were not statistically significant, and there were higher background levels in the assay (Fig. S8). The convalescent control is a pool of 3 human convalescent serum samples (Nexelis). Two animals in the MV-014-212 group with the higher serum nAb titers (Fig. 5B) were chosen to compare to this convalescent pool control. As with the pseudovirus assay (Fig. S8), the microneutralization assay showed that the NT50 of the AGM sera were approximately 4-fold lower than the human convalescent pool (Fig. 5C). Lastly, the serum of one AGM vaccinated with MV-014-212, (the animal showing the highest titers in Fig. 5C) was used in a conventional 50% plaque-reduction neutralization assay with SARS-CoV-2 in BSL-3 containment (Muruato 2020, Liu 2021). In this assay, the neutralizing titers (PRNT50) against SARS-CoV-2 virus or the two variants of concern, B.1.351 and B.1.17 were determined (Fig. 5D). The results showed that vaccination with MV-014-212 elicits neutralizing activity against the wt strain and both variants of concern (the pre-immune serum titers were below the limit of detection for all the virus strains tested, data not shown). The neutralization titer of B.1.351 was equivalent to that of the *wt* strain and B.1.1.7 showed slightly higher neutralizing titers. Taken together, the data suggested that MV-014-212 elicited modest serum neutralizing antibody titers in AGMs, and there was cross neutralization against the variants B.1.351 and B.1.17.

MV-014-212 elicits a Th1-biased cellular immune response in hACE2-mice

Mouse models of vaccine-associated enhanced respiratory disease (VAERD) suggest that an imbalance in type 1 (Th1) and type 2 (Th2) T helper cell immunity with a skewing towards Th2 response contributes to enhanced lung pathology following challenge (Boelen 2000). To assess the balance of Th1 and Th2 immunity generated after vaccination with MV-014-212, transgenic mice expressing human ACE-2 receptor were inoculated with a single dose of MV-014-212 or PBS by the intranasal route. A control group received an intramuscular prime and boost vaccination with SARS-CoV-2 spike protein formulated in alum, which has been shown to skew immunity towards a Th2 response (Corbett 2020). On Day 28, serum was collected to measure total spike-specific IgG, IgG2a and IgG1 by ELISA. In addition, spleens were collected and the number of splenocytes expressing interferon-γ (IFNγ) or IL-5 were measured by ELISpot assay. The ratio of IgG2a/IgG1 and the ratio of cells producing IFNγ/IL-5 are indicators of Th1-biased cellular immune response (Corbet 2020, van der Fits 2020).

The results showed that MV-014-212 induced spike-reactive splenocytes as measured by ELISpot assay (Fig. 6A). Importantly, MV-014-212 induced higher numbers of splenocytes expressing IFNγ relative to IL-5 when cell suspensions were stimulated with a spike peptide pool suggesting that vaccination with MV-014-212 produced a Th1-biased immune response. The ratio of IFNγ producing cells to IL-5 producing cells in the MV-014-212 group was more than one order of magnitude higher than in the group vaccinated with alum-adjuvanted spike protein, (Fig. 6B). Consistent with the ELISpot data, the ratios of IgG2a/IgG1 detected in serum were higher in the animals vaccinated with MV-014-212 than the control group vaccinated with alum-adjuvanted spike (Fig. 6C and 6D). These data suggest that intranasal vaccination with live attenuated, recombinant MV-014-212 induced a Th1-biased antiviral immune response.

Discussion

MV-014-212 is a recombinant live attenuated COVID-19 vaccine designed to be administered intranasally to stimulate mucosal as well as systemic immunity against SARS-CoV-2. MV-014-212 was engineered to express a functional SARS-CoV-2 spike protein in place of the RSV membrane surface proteins F, G and SH in an attenuated RSV strain expressing codon deoptimized NS1 and NS2 genes. Indeed, replication of MV-014-212 was attenuated in the respiratory tract of AGM following mucosal administrations in the nose and trachea and it elicited SARS-CoV-2 spike-specific mucosal IgA and serum IgG. Furthermore, vaccination with MV-014-212 induced a modest level of serum neutralizing antibodies and, more importantly, a single administration of the Meissa COVID-19 vaccine provided robust protection against SARS-CoV-2 challenge in AGM.

Based on the levels of viral sgRNA detected after SARS-CoV-2 challenge, the efficacy of MV-014-212 after one dose in NHPs is comparable to that reported for efficacy of the current EUA vaccines in NHPs. The efficacy and kinetics of clearance in MV-014-212 vaccinated AGMs is comparable to those observed after two doses of BNT126b2 or mRNA1273 (Vogel 2021, Corbett- N Eng J Med. 2020) in nasal swabs and BAL of rhesus macaques. hAdOx1 nCoV-19, on the other hand, confers comparable protection in the BAL but is less protective the in nose of rhesus monkeys (van Doremalen 2020), compared to MV-014-212. The dose of the challenge virus reported in the Ad26-CoV2.S vaccine NHP study (Mercado 2020) was approximately 170 times lower that the one used in this study, confounding a direct comparison of the results. The mRNA and other non-replicating COVID vaccines were evaluated in Rhesus monkeys which are less permissive for RSV replication than AGMs (Taylor 2017). AGMs were selected as the model for evaluating the attenuation and immunogenicity of MV-014-212 because they support both RSV (Taylor 2017) and SARS-CoV-2 (Woolsey 2021, Cross 2020, Blair 2021, Lee 2021) replication. The level of SARS-CoV-2 detected in the mock-treated AGMs in this study was as high or higher than the levels reported for the mock groups in other vaccine studies (van Doremalen 2020, Corbett- N Eng J Med. 2020, Vogel 2021), allowing comparison of the results between different monkey species.

The use of a semi permissive animal model for the evaluation of the live attenuated vaccine (LAV) candidate MV-014-212 constitutes a limitation of this study, since LAVs rely on replication to elicit a robust immune response. The semi-permissivity of AGMs to RSV and SARS-CoV-2 would result in lower replication of MV-014-212 and a more modest serum neutralizing antibody response. In a more permissive host like humans, MV-014-212 is expected to replicate to higher titers potentially resulting in higher immunogenicity than that observed in AGMs.

Remarkably, immunization of AGM with MV-014-212 resulted in both mucosal and systemic antibody responses. There was approximately 100-fold more spike-specific total serum IgG in MV-014-212 vaccinated AGM compared to AGM that received *wt* RSV A2 or PBS inoculations. Spike-specific IgA was also detected in nasal swabs of MV-014-212 immunized animals. There

was approximately an 8-fold increase in IgA concentration 25 days following vaccination with MV-014-212. In an experimental human challenge study, low RSV F-specific mucosal IgA was a better predictor for susceptibility to RSV challenge in seropositive adults than serum IgG and neutralizing antibody levels (Habibi 2015). Indeed, spike RBD-specific dimeric serum IgA was shown to be more potent at neutralizing SARS-CoV-2 than monomeric IgG (Wang 2021). By inference, secretory IgA which exists at mucosal surfaces as dimeric IgA may act as a potent inhibitor of SARS-CoV-2 at the site of infection. Interestingly, IgA antibodies dominate early humoral responses in human SARS-CoV-2 infections and IgA plasmablasts with mucosal homing potential peaked during the third week of disease onset (Sterlin 2021).

A SARS-CoV-2 neutralizing antibody response was detected in the serum of vaccinated AGMs in a microneutralization assay using an mKate2-expressing MV-014-212 virus (MVK-014-212). This response was also observed in a luciferase-based pseudovirus assay and in a conventional plaque reduction assay with SARS-CoV-2. The plaque reduction assay also detected a neutralizing response against two variants of concern, B.1.351 and B.1.1.7, with comparable titers to the ones detected against the USA-WA2020 strain. Direct comparison of the AGM serum nAb titers to serum nAb titers published for non-replicating vaccines in rhesus monkeys or to titers in human convalescent sera is confounded by the semi-permissivity of AGM for MV-014-212 replication. The immunogenicity of MV-014-212 is being studied in an ongoing Phase 1 of clinical trial.

The IM-administered EUA vaccines currently in use offer very satisfactory levels of protection but their ability to prevent asymptomatic transmission is still unclear (reviewed by Tiboni et al., 2021). Vaccines delivered intranasally stand a higher chance of eliciting local mucosal immunity preventing not only systemic infection but also local replication and shedding. Indeed, IN-delivered MV-014-212 resulted in the production of spike-specific IgA in the nose of AGMs. According to the July 6th, 2021 "The Landscape of candidate vaccines in clinical development" prepared by WHO, there are eight intranasal COVID-19 vaccines in clinical trials (Table 1). Further development of one of these candidates, AdCOVID from Altimmune, was very recently discontinued (Press Release from Altimmune, https://ir.altimmune.com/news-releases/news-release-details/altimmune-announces-update-adcovidtm-phase-1-clinical-trial). Of the remaining programs, only MV-014-212 and COVI-VAC (Codagenix) are live attenuated viruses. Unlike COVI-VAC, MV-014-212 is a non-segmented negative strand RNA virus not prone to recombine in nature. RNA recombination is extremely rare for non-segmented negative strand RNA viruses outside of experimental co-infections in laboratory settings (Spaan 2003, Han 2011, Tan 2012). In addition to the lack of natural recombination, the results presented in this study showed that MV-014-212 was genetically stable. Neither accumulation of mutations nor loss of the furin cleavage site was detected when the virus was serially passaged ten times in Vero cells. This contrasts with another recombinant live viral COVID-19 vaccine based on the VSV backbone (Yahalom-Ronen 2020) where mutations arose at passage 9 in Vero E6 cells. One of these mutations occurred in the multi-basic S1/S2 furin cleavage site and another generated a stop codon that resulted in a 24-amino acid truncation of the spike cytoplasmic tail. Truncation of the spike cytoplasmic tail was

also reported when *wt* SARS-CoV-2 (Ou 2020) or pseudotyped SARS-CoV-2 (Case 2020, Dieterle 2020) were propagated in tissue culture. MV-014-212 virus shed from vaccinated AGMs had no mutations in the spike gene. Therefore, the chimeric spike gene in MV-014-212 appears to have a stable genotype *in vitro* and *in vivo.*

The vaccine profile of MV-014-212 remains unique among the current COVID-19 vaccines that have emergency use authorization or are in clinical development. MV-014-212 is administered intranasally, a needle-free route that offers potential advantages for global immunization. The intranasal route is similar to the natural route of infection of SARS-CoV-2 and generates both mucosal and humoral immune responses in AGMs without any adjuvant formulation. Modeling based on yields from production of Phase 1 clinical study material projected a potential dose output of hundreds of millions of doses per annum in a modestly sized facility using high intensity bioreactor systems. Mucosally delivered live attenuated vaccines such as MV-014-212 entails minimum downstream processing and has an anticipated low cost of goods. In addition, needle-free delivery reduces supply risks. Overall, MV-014-212 is well-suited for domestic and global deployment as a primary vaccine or as a heterologous booster. MV-014-212 is currently being evaluated as a single dose intranasal vaccine in a Phase 1 clinical trial (NCT04798001).

Materials and Methods

Cells, viruses, and animals

Vero RCB1 (WHO Vero RCB 10-87) cells were grown in minimal essential medium (MEM, Gibco) containing 10% fetal bovine serum (FBS, Corning) and 1X Corning Antibiotic/Antimycotic mix consisting of 100 I.U./mL Penicillin, 100 µg/mL Streptomycin 0.25 µg/mL Amphotericin with 0.085 g/L NaCI. RCB2 Cells were derived from RCB1 and adapted to grow in serum-free media. RCB2 cells used in this study were grown in serum-free medium OptiPro (Gibco) supplemented with 4 mM of L-glutamine (Gibco). Both Vero cell lines were cultured at 37℃, 5% CO2 with 95% humidity.

African green monkeys (*Chlorocebus aethiops*) were obtained from St. Kitts and were of indeterminate age weighing 3-6 kg. The monkeys were screened and verified to be seronegative for RSV and SARS-CoV-2 by an RSV microneutralization assay and spike SARS-CoV-2 ELISA (BIOQUAL). Animals also underwent a physical examination by the veterinary staff to confirm appropriate health status prior to study. Each AGM was uniquely identified by a tattoo. One male and 3 females were assigned to the MV-014-212 and RSV groups. 2 females and 1 male were assigned to the Mock group. Cage-side observations included mortality, moribundity, general health and signs of toxicity. Clinical observations included skin and fur characteristics, eye and mucous membranes, respiratory, circulatory, autonomic and central nervous systems, somatomotor, and behavior patterns. The body weight of each monkey was recorded before the start of the dosing period and at each time of sedation. Consistent with the overall low levels of MV-014-212 replication in the respiratory tract of AGMs, no adverse events that were considered treatment-related were observed following inoculation with the vaccine. On Day 16 post-vaccination one monkey inoculated with MV-014-212 died unexpectedly. Death occurred 4 days after the last NS and BAL surgical sample collection. A definitive determination of the cause of death could not be ascertained based on macroscopic or microscopic postmortem evaluations; however, there was no evidence that suggests the death was vaccine related. Moreover, the deceased animal had the lowest titer in NS samples compared to the other animals in this treatment group with only one swab containing virus that was above the detection limit of the plaque assay (50 PFU/mL), and no detectable infectious virus in BAL at any of the time points evaluated.

Male and female K18-hACE2 Tg (strain #034860, B6.Cg-Tg[K18-ACE2]2Prlmn/J) mice were procured from The Jackson Laboratory (Bar Harbor, ME) and were approximately 8-10 weeks old at the time of vaccination.

The animal studies were conducted in compliance with all relevant local, state, and federal regulations and were approved by the BIOQUAL Institutional Animal Care and Use Committee (IACUC).

RSV Memphis37b was kindly provided by hVIVO (United Kingdom) and RSV TN12/11-19, by R.S. Peebles Jr (Vanderbilt University Medical Center).

Plasmid construction

The recombinant MV-014-212 and derived viruses were cloned in the antigenome orientation in bacterial artificial chromosomes (BAC) under the control of the T7 polymerase promoter (Hotard 2012). The BACs containing the recombinant MV-014-212 and MVK-014-212 sequences were constructed by restriction digestion and ligation from the DB1-QUAD and kRSV-DB1-QUAD plasmids (encoding the antigenome of an attenuated version of RSV with or without the mKate gene, respectively, Rostad 2018). The DNA sequence encoding the chimeric spike protein was designed to contain compatible cloning sites and it was synthesized by Twist Biosciences. The kRSV-DB1-QUAD plasmid and spike insert were digested with the enzymes AatII and SalI (NEB) and ligated with T4 DNA ligase (NEB) overnight at 16 °C. Stabl3 chemically competent cells (Invitrogen) were transformed with the ligation mix and selected for chloramphenicol resistance for 20-24 hours at 32°C. MV-014-212 BAC was derived from the MVK-014-212 vector by removing the fragment between the KpnI and AatII restriction sites (~7kb containing the mKate gene) and replacing it with the corresponding fragment extracted from DB1-QUAD by restriction digestion and ligation. For all the constructs, the sequences of the entire encoded viruses were confirmed via Sanger sequencing. The construction of the plasmid rA2-mkate (a.k.a. kRSV-A2) was described in Rostad 2016.

Virus rescue and harvest

Vero cells were electroporated with the bacterial artificial chromosome (BAC) encoding MV-014-212 (or the reporter virus) together with helper plasmids based on the pCDNA3.1 vector encoding the RSV proteins N, P, M2-1 and L, and the T7 polymerase under the control of a CMV promoter (Hotard 2021). The cells were recovered in SFM-OptiPro medium supplemented with 4mM glutamine and 10% fetal bovine serum (Hyclone) for 2 passages and then expanded in serum free medium with glutamine until CPE was extensive.

The recombinant viruses were harvested in Williams E medium (Hyclone) supplemented with Sucrose Phosphate Glutamate Buffer (SPG) or SPG alone by scraping the infected cells directly into the media. The lysate was vortexed for 15 seconds at maximum speed (3200 rpm) to release the viral particles and flash frozen. One cycle of thawing and vortexing was performed to increase the release of virus before the stocks were aliquoted, flash-frozen and stored at -70 °C until use.

Plaque assay

Plaque assays for all the viruses used were performed in 24-well plates on Vero cells. Cells at 70% confluence were inoculated with 100 µl of 10-fold serial dilutions of viral samples (10^{-1} to 10^{-6}). Inoculation was carried out at room temperature with gentle rocking for 1 h before adding 0.75% methylcellulose (Sigma) dissolved in MEM supplemented with 10% FBS (Corning) and 1X Corning Antibiotic/Antimycotic mix. Cells were incubated for 4-5 days at 32℃ before fixing in methanol and immunostaining. For MV-014-212 and MVK-014-212, we used Rabbit anti-SARS-CoV-2 spike polyclonal antibody (Sino Biological) and Goat anti-rabbit HRP-conjugated secondary antibody (Jackson ImmunoResearch). For rA2-mKate2, the reagents used were Goat anti-RSV primary antibody (Millipore) and Donkey anti-goat HRP-conjugated secondary antibody (Jackson ImmunoResearch). In all cases, the viral plaques were stained with AEC (Sigma). The limit of detection is 1 PFU per well, corresponding to a minimum detectable titer of 100 PFU/ml.

RNA sequencing

RNA from MV-014-212 samples was extracted using QIAamp® Viral RNA Mini Kit following the protocol suggested by the manufacturer (Qiagen). The quality and concentration of the extracted RNA were evaluated by gel electrophoresis and UV spectrophotometry. The extracted RNA was used as the template for reverse transcription (RT) using Invitrogen SuperScript® IV First-Strand Synthesis System using a specific primer or random hexamers. The cDNA 2nd strand was synthesized with the Platinum™ SuperFi™ PCR Master Mix. The purified PCR products were directly sequenced using the BigDye® Terminator v3.1 Cycle Sequencing Kit (Applied Biosystems). The sequencing reactions were purified using Sephadex G-50 purification and analyzed on ABI 3730xl DNA Analyzer. The sequence traces were assembled using Sequencher software and the assembly was manually confirmed. The RNA sequencing for this study was performed by Avance Biosciences Inc., Houston TX.

Western Blot

Viruses and control recombinant SARS-CoV-2 spike protein (LakePharma, San Carlos, CA) were denatured with Laemmli sample buffer (Alfa Aesar, Ward Hill, MA) by heating at 95 ºC for 10 minutes. Proteins were separated by SDS-PAGE in a 4-15% gradient gel and transferred to PVDF membranes using a transfer apparatus according to the manufacturer's protocol (BIO-RAD, Hercules, CA). After transfer, blots were washed in deionized water and probed using the iBind Flex system according to the manufacturer's protocol (Invitrogen, ThermoFisher). Rabbit anti-SARS-CoV-2 spike (Sino Biological Inc, Beijing, China) was diluted in iBind solution (Invitrogen, Carlsbad, CA) at 1:1000. HRP conjugated anti-Rabbit IgG (Jackson ImmunoResearch, Philadelphia, PA) was diluted in iBind Solution at 1:5000. Blots were washed in deionized water

and developed with ECL system (Azure Biosystems, Dublin, CA) according to manufacturer's protocol. The blots were stripped with Restore Western Blot Stripping Buffer (ThermoFisher, Carlsbad, CA) and reprobed with goat anti-RSV polyclonal antisera (Sigma-Aldrich, St. Louis, MO) and a monoclonal antibody specific for GAPDH (6C5) protein (ThermoFisher, Carlsbad, CA).

Plaque assay for detecting virus shedding in AGMs

Nasal swabs (NS) and bronchoalveolar lavage (BAL) samples were collected and stored on ice until assayed for vaccine shedding by plaque assay. Vero cells were seeded in 0.5 mL per well at 1 x 10^5 cells/mL in culture media in 24 well plates. The plates were incubated overnight at 37°C in a humid incubator containing 5% CO_2. The samples were diluted in DMEM without serum by adding 30 µL of nasal swab or BAL to 270 µL of DMEM. A total of six 10-fold serial dilutions were prepared in DMEM from 10^{-1} to 10^{-6}. The media was removed from the 24 well plate and 100 µL of each dilution was added to duplicate wells of the 24 well plate of Vero cells. The plate was incubated at room temperature with constant rocking on a Rocker 35EZ, Model Rocker 35D (Labnet, Edison, NJ) for 1 h. At the end of this incubation, 1 mL of methyl cellulose media (MEM supplemented with 10% fetal bovine serum, 1x antibiotic/antimycotic, and 0.75% methyl cellulose) was added to each well. The plate was incubated at 34 ºC for 6 days in a humid incubator containing 5% CO_2.

The plaques were visualized by immunostaining using RSV or SARS-CoV-2 antibodies. For immunostaining, the methyl cellulose media was aspirated, and the cell monolayers were washed with 1 mL of PBS at room temperature. The PBS was removed, and the cells were fixed by the addition of 1 mL of methanol to each well and the plate was incubated at room temperature for 15 minutes. The methanol was removed, and cells washed with 1 mL of PBS followed by the addition of 1 mL Blotto solution (5% non-fat dried milk in Tris-buffered saline, Thermo-Fisher). The plates were incubated at room temperature for 1 h. The Blotto solution was removed, and 0.25 mL of primary goat anti-RSV polyclonal antibodies (Millipore, Hayward, CA) diluted 1 to 500 in Blotto was added to RSV infected cells. Cells infected with MV-014-212 were stained with primary rabbit anti-SARS-CoV-2 spike protein polyclonal antisera (Sino Biologicals, Beijing, CN). The plates were incubated for 1 h at room temperature with constant rocking. Primary antibodies were removed, and wells were washed with 1 mL Blotto solution.

For RSV infected cells, 0.25 mL of donkey anti-goat HRP-conjugated polyclonal antisera (Jackson ImmunoResearch, West Grove, PA) diluted 1:250 in Blotto was added to each well. For MV-014-212 infected cells goat anti-rabbit HRP-conjugated polyclonal antisera (Jackson ImmunoResearch, West Grove, PA) diluted 1:250 in Blotto was added to each well. The pate was incubated for 1 h at room temperature with constant rocking. After incubation, the secondary antibodies were removed, and the wells washed with 1 mL of PBS. Developing solution was prepared by diluting

AEC substrate 1 to 50 in 1x AEC buffer solution. A total of 0.25 mL of developing solution was added to each well and the plate was incubated at room temperature for 15 to 30 minutes with constant rocking until red immunostained plaques were visible. The developing reaction was terminated by rinsing the plate under tap water. The plaques were enumerated, and titers were calculated.

RT-qPCR of SARS-CoV-2 subgenomic RNA for detecting shedding of challenge virus

The standard curve was prepared from frozen RNA stocks and diluted to contain 10^6 to 10^7 copies per 3 µL. Eight 10-fold serial dilutions of control RNA were prepared using RNAse-free water to produce RNA concentrations ranging from 1 to 10^7 copies/reaction.

The plate was placed in an Applied Biosystems 7500 Sequence detector and amplified using the following program: 48 °C for 30 minutes, 95 °C for 10 minutes followed by 40 cycles of 95 °C for 15 seconds, and 1 minute at 55 °C. The number of copies of RNA per mL of sample was calculated based upon the standard curve.

Total RNA from tissues was extracted using RNA-STAT 60 (Tel-test"B")/ chloroform followed by precipitation of the RNA and resuspension in RNAse-free water. To detect SARS-CoV-2 sgRNA, a primer set and probe were designed to detect a region of the leader sequence and E gene RNA from SARS-CoV-2. The E gene mRNA is processed during replication to contain a 5' leader sequence that is unique to sgRNA (not packaged into the virion) and therefore can be used to quantify sgRNA. A standard curve was prepared using known quantities of plasmid DNA containing the E gene sequence including the unique leader sequence to produce a concentration range from 1 to 10^6 copies/reaction. The PCR reactions were assembled using 45 µL master mix (Bioline, Memphis, TN) containing 2X buffer, Taq-polymerase, reverse transcriptase and RNAse inhibitor. The primer pair was added at 2 µM. 5 µL of the sample RNA was added to each reaction in 96-well plate. The PCR reactions were amplified in an Applied Biosystems 7500 Sequence detector using the following conditions: 48 °C for 30 minutes, 95 °C for 10 minutes followed by 40 cycles of 95 °C for 15 seconds, and 1 minute at 55 °C.

Primers / Probe sequences are shown below:

SG-F: CGATCTTGTAGATCTGTTCCTCAAACGAAC

SG-R: ATATTGCAGCAGTACGCACACACA

FAM-ACACTAGCCATCCTTACTGCGCTTCG-BHQ

TCID50 assay to detect shedding of SARS-CoV-2 in BAL and NS of AGMs after challenge

Vero TMPRSS2 cells (obtained from Adrian Creanga, Vaccine Research Center-NIAID) were plated at 25,000 cells/well in DMEM + 10% FBS + Gentamicin and the cultures were incubated at 37°C, 5.0% CO2. Cells were 80 -100% confluent the following day. Medium was aspirated and replaced with 180 µL of DMEM + 2% FBS + gentamicin. Twenty (20) µL of sample was added to top row in quadruplicate and mixed using a P200 pipettor 5 times. Using the pipettor, 20 µL was transferred to the next row, and repeated down the plate (columns A-H) representing 10-fold dilutions. Positive (virus stock of known infectious titer in the assay) and negative (medium only) control wells were included in each assay set-up. The plates were incubated at 37°C, 5.0% CO_2 for 4 days. The cell monolayers were visually inspected for CPE. The TCID50 value was calculated using the Read-Muench formula.

SARS-CoV-2 total IgG ELISA for AGM sera

MaxiSorp immuno plates (Thermo-Fisher, Waltham, MA) were incubated overnight at 4 ºC with 100 µL of 0.65 µg/mL of SARS-CoV-2 spike prepared in PBS (Pre-S SARS-CoV-2 spike, Nexelis). The protein solution was removed, and the plate was washed 4 times with 250 µL of PBS supplemented with 0.05% Tween 20 (PBST). Blocking solution (PBST containing 5% non-fat dried milk) was added at 200 µL per well and the plate was incubated for 1 h at room temperature. A SARS-CoV-2 spike specific IgG (Nexelis) was diluted in blocking solution and used as a standard. Negative control serum was diluted 1:25 in blocking solution. Serum samples were diluted at 1:25 followed by eight 2-fold serial dilutions in blocking solution. The blocking solution was removed from the plate and the wells washed once with 250 µL of PBST followed by addition of 100 µL of the diluted serum samples and controls and the plate was incubated for 1 h at room temperature. The plate was washed 4 times with 250 µL PBST and 100 µL of HRP-conjugated goat anti-monkey IgG antibody (PA1-8463, Thermo Fisher, Waltham, MA) diluted in blocking solution was added to each well following the last wash step. The plate was incubated for 1 h at room temperature and then washed 4 times in 250 µL PBST. Developing solution containing 3, 3', 5, 5' - Tetramethylbenzidine (TMB) substrate (1-Step Ultra TMB-ELISA Substrate Solution, ThermoFisher) was added to each well and the plate was incubated at room temperature for 30 minutes to allow the color to develop. The colorimetric reaction was terminated by the addition of 100 µL of ELISA Stop Solution (Invitrogen). The absorbance at 450 nm and 650 nm was read by spectrophotometry using a SpectraMax iD3 microplate reader (Molecular Devices, San Jose, CA).

SARS-CoV-2 IgA ELISA for AGM nasal swabs

Purified pre-fusion SARS-CoV-2 spike antigen (LakePharma) was adsorbed onto 96-well MaxiSorp immuno microplate (Thermo-Fisher). The positive control was a serum pool from three COVID-19 convalescent individuals (Nexelis). Total IgA purified from human serum was used as a standard (Sigma-Aldrich, St. Louis, MO). To generate the IgA standard curve anti-human IgA capture antibodies Mab MT57 (MabTech) were absorbed on plates instead of spike antigen. Following incubation, the microplate was washed 4x with 250 µL PBST and blocked with 1% BSA in PBST. Purified human IgA standard, controls or sample dilutions were then added and incubated in the coated microplate to allow binding. The plates were washed and a biotinylated goat anti-human IgA antibody (Mabtech) with cross reactivity to monkey antibodies was added to all wells. Excess biotinylated anti-IgA antibody was removed by washing and streptavidin-conjugated HRP (Southern Biotech) was added. TMB was added and color development was stopped by addition of stop solution from Invitrogen. The absorbance of each well was measured at 450 nm. The standard total IgA antibody assayed on each test plate was used to calculate the concentration of IgA antibodies against spike protein in the AGM samples expressed in the arbitrary units ELU/mL. The measurements were performed in duplicates and average values are reported with standard deviations.

Microneutralization assay

Heat-inactivated sera from the AGMs were diluted serially in MEM with non-essential amino acids (Gibco) and antibiotics/antimycotic. All experiments were done in duplicate. 200 PFU of the desired reporter virus were added to each dilution and incubated at room temperature for one hour. Confluent RCB1 cells grown in a clear-bottom black 96-well plate (Grenier) were infected with the serum-virus mixes and centrifuged (spinoculated) at 1,800 x g for 30 minutes at 20 °C. The plates were incubated for 20 h at 37 °C and 5% CO_2. The fluorescent foci in each well were counted using a Celigo Image Cytometer (Nexcelom) and converted to %Inhibition using the formula below

$$\%\ \textbf{inhibition} = 100 \times \left[1 - \frac{(L - MIN)}{(MAX - MIN)}\right]$$

where MIN is the average number of foci obtained in the control wells with only cells (no virus) and MAX is the average number of foci from the wells in the control wells with only virus (no serum). L is the number of foci in the sample wells. The resulting curves of inhibition vs. dilution of the sera were fitted using non-linear regression, option "[inhibitor] vs normalized response-

variable slope" in GraphPad Prism (version 9.0.0). From the fitting, IC50 was obtained and NT50 was calculated as the reciprocal of IC50.

Pseudovirus neutralization assay

SARS-CoV-2 Spike ΔCT protein-bearing vesicular stomatitis virus (VSV) pseudotyped particles in which the VSV glycoprotein G gene was replaced by the luciferase reporter gene were purchased from Nexelis, and the assay was performed at Meissa. Starting with a dilution of 1/25, serial 2-fold dilutions of heat-inactivated AGM sera were incubated with the pseudotyped viral particles (3 x 10^5 RLU/well) at 37°C for one hour after which the mixes were used to infect Vero E6 monolayers in white 96-well plates. The cells were incubated with the infection mixes for 20 ± 2 hours at 37°C with 5% CO2. The medium was then discarded, and the cells were lysed in ONE-GloTM EX Luciferase Reagent (Promega). The lysis and luciferase reactions were allowed to proceed for 3 minutes at room temperature with shaking at 600 rpm and luminescence was read with a SpectraMax i3D plate reader. The values of luminescence were converted to percentage of inhibition using the equation shown in the previous paragraph where MIN is the average of reads obtained in the cell-only wells and MAX is the average of the reads from the wells of the pseudovirus-only control. L is the sample luminescence value. The inhibition vs. dilution curves were fitted using nonlinear regression, option "[inhibitor] vs normalized response-variable slope" in GraphPad Prism (version 9.0.0). From the fitting IC50 was obtained and NT50 was calculated as the reciprocal of IC50.

Plaque reduction neutralization test

A conventional 50% plaque-reduction neutralization test (PRNT50) was performed to quantify the serum-mediated virus suppression as previously reported (Muruato 2020). Briefly, individual sera were 2-fold serially diluted in culture medium with a starting dilution of 1:40 (dilution range of 1:40 to 1:1280). The diluted sera were incubated with 100 PFU of USA-WA1/2020 or mutant SARS-CoV-2. After 1 h incubation at 37 °C, the serum-virus mixtures were inoculated onto a monolayer of Vero E6 cells pre-seeded on 6-well plates on the previous day. A minimal serum dilution that suppresses >50% of viral plaques is defined as PRNT50.

All recombinant SARS-CoV-2s with spike mutations (Liu 2021) were prepared on the genetic background of an infectious cDNA clone derived from clinical strain USA-WA1/2020 (Xie 2020).

Spike-specific IgG1 and IgG2a ELISA

Serum samples from mice were collected on Day -21 and on Day 28 post vaccination to quantify the levels of SARS-CoV-2 spike-specific IgG1 and IgG2a antibodies by ELISA. Purified perfusion-stabilized SARS-CoV-2 spike protein (SARS-CoV-2/human/USA/WA1/2020, from LakePharma) was diluted to 1 µg/mL in PBS and 100 µL was added to each well of a Maxisorp immuno plates (Thermo-Fisher) and incubated overnight at 4ºC. The plate was washed 4 times in PBST (PBS+0.05% Tween 20) and 100 µL of blocking solution (PBST + 2% BSA) was added to each well and the plate was incubated for 1 hour at room temperature. Serum dilutions were prepared in blocking solution with the first dilution at 1:25 for the IgG1 assay or 1:10-1:100 for the IgG2a assay. SARS-CoV-2 spike IgG1 (Sino Biological) or anti-spike-RBD-mIgG2a (InvivoGen) were diluted in blocking solution and used as standards for the assay.

The blocking solution was removed and 100 µL of diluted antibody were added to each well. The plate was incubated at room temperature for 1 h and then washed 4 times in PBST using the plate washer. Then, 100 µL of HRP-conjugated goat-anti-mouse IgG1 (Thermo Fisher) or HRP-conjugated goat-anti-mouse IgG2a (Thermo Fisher) secondary antibodies diluted 1:32,000 and 1:1000, respectively, were added to each well and the plate was incubated at room temperature for 1 h. The plate was washed 4 times in PBST. 100 µL of 1-step ultra TMB-ELISA substrate solution (Thermo Fisher) was added to each well and the plate incubated for 30 min with constant rocking on an orbital shaker. After the incubation period, 100 µL of stop solution (Invitrogen) was added to each well and the plate read on a Spectramax id3 plate reader (Molecular Devices) at 450 nm and 620 nm.

ELISPOT of splenocytes from MV-014-212 vaccinated hACE2-mice

Spleens from vaccinated ACE-2 mice were collected on Day 28 post-inoculation and stored in DMEM containing 10% FBS on ice until processed. The spleens were homogenized on a sterile petri dish containing medium. The homogenate was filtered through a 100 µm cell strainer and the cell suspension transferred to a sterile tube on ice. The cells were collected by centrifugation at 200 x g for 8 min at 4ºC. The supernatant was removed and residual liquid on the edge of the tube blotted with a clean paper towel. Red blood cells were lysed by resuspending the cell pellet in 2 mL of ACK lysis buffer (155 mM ammonium chloride, 10 mM potassium bicarbonate, 0.1 mM EDTA) and incubating the samples at room temperature for approximately 5 min. PBS was added at 2X to 3X of the volume of cell suspension and cells were collected by centrifugation at 200 x g for 8 min at 4 ºC. The cell pellet was washed twice in PBS and the cells collected by centrifugation at 200 x g for 8 min at 4 °C. The supernatant was removed, and the pellet resuspended in 2mM L-Glutamine CTL-Test Media (Cell Technology Limited, OH, USA). The suspension was filtered through a 100 µm cell strainer into a new 15 mL conical tube and the cells counted using a

hemocytometer and resuspended at the appropriate cell concentration. Cells were maintained at 37 ºC in a humidified incubator with 5% CO_2 until used in the ELISpot assay.

The ELISpot assay was performed using a mouse IFNγ/IL-5 Double-Color ELISPOT assay kit (Cell Technology Limited, OH, USA). Murine IFNγ/IL-5 Capture Solution and 70% ethanol was prepared according to the manufacturer's protocol (Cell Technology Limited, OH, USA). The membrane on the plate was activated by addition of 15 µL of 70% ethanol to each well. The plate was incubated for less than one minute at room temperature followed by addition of 150 µL PBS. The underdrain was removed to drain the solution in the wells and each well was washed twice with PBS. Murine IFNγ/IL-5 Capture Solution (80 µL) was added to each well and the plate was sealed with parafilm and incubated at 4 ºC overnight. The Capture Solution was removed, and the plate washed one time with 150 µL PBS. A peptide pool containing peptides of 15 amino acids in length that span the SARS-CoV-2 spike protein (PepMix™ SARS-CoV-2 spike Glycoprotein, JPT Peptide Technologies, Berlin DE) were prepared at 10 mg/mL and 100 µL was added to each well. A positive control containing Concanavalin A (Con A) mitogen (10 µg/mL) was added to a separate reaction mixture. The splenocytes were mixed with CTL-Test™ Medium (Cell Technology Limited, OH, USA) to yield a final cell density of 3,000,000 cells / mL and 100 µL/well were added to the plate using large orifice tips. The plate was incubated at 37 ºC in a humidified incubator containing 9% CO_2 for 24 hours. The plates were washed twice with PBS and then twice with 0.05% Tween-PBS at a volume of 200 µL/well for each wash followed by addition of 80 µL/well anti-murine IFNγ/IL-5 Detection Solution (Cell Technology Limited, OH, USA). The plates were incubated at room temperature for two hours. The plate was washed three times with PBST at 200 µL/well for each wash followed by the addition of 80 µL/well of Tertiary Solution (Cell Technology Limited, OH, USA). The plates were incubated at room temperature for one hour. The plate was washed twice with PBST, and then twice with 200 µL/well of distilled water. Blue Developer Solution (Cell Technology Limited, OH, USA) was added at 80 µL/well and the plate will be incubated at room temperature for 15 min. The plate was rinsed three times in tap water to stop the developing reaction. After the final wash, Red Developer Solution (Cell Technology Limited, OH, USA) was added at 80 µL/well and the plate was incubated at room temperature for 5-10 min. The plate was rinsed three times to stop the developing reaction. The plate was air-dried for 24 hours face down on paper towels on the bench top. The spots on the plate representing splenocytes expressing IFN-γ (red) or IL-5 (blue) were quantified using the CTL-Immunospot plate reader (ImmunoSpot 7.0.23.2 Analyzer Professional DC\ImmunoSpot 7, Cellular Technology Limited) and software (CTL Switchboard 2.7.2).

References

1. Wu F, Zhao S, Yu B, Chen YM, Wang W, Song ZG, Hu Y, Tao ZW, Tian JH, Pei YY, Yuan ML, Zhang YL, Dai FH, Liu Y, Wang QM, Zheng JJ, Xu L, Holmes EC, Zhang YZ. A new coronavirus associated with human respiratory disease in China. Nature. 2020 Mar;579(7798):265-269. doi: 10.1038/s41586-020-2008-3. Epub 2020 Feb 3. Erratum in: Nature. 2020 Apr;580(7803):E7. PMID: 32015508; PMCID: PMC7094943.

2. Zhou P, Yang XL, Wang XG, Hu B, Zhang L, Zhang W, Si HR, Zhu Y, Li B, Huang CL, Chen HD, Chen J, Luo Y, Guo H, Jiang RD, Liu MQ, Chen Y, Shen XR, Wang X, Zheng XS, Zhao K, Chen QJ, Deng F, Liu LL, Yan B, Zhan FX, Wang YY, Xiao GF, Shi ZL. A pneumonia outbreak associated with a new coronavirus of probable bat origin. Nature. 2020 Mar;579(7798):270-273. doi: 10.1038/s41586-020-2012-7. Epub 2020 Feb 3. PMID: 32015507; PMCID: PMC7095418.

3. WHO Director-General's opening remarks at the media briefing on COVID19 -March 2020-https://www.who.int/director-general/speeches/detail/who-director-general-s-opening-remarks-at-the-media-briefing-on-covid-19---11-march-2020)

4. Coronaviridae Study Group of the International Committee on Taxonomy of Viruses. The species Severe acute respiratory syndrome-related coronavirus: classifying 2019-nCoV and naming it SARS-CoV-2. Nat Microbiol. 2020 Apr;5(4):536-544. doi: 10.1038/s41564-020-0695-z. Epub 2020 Mar 2. PMID: 32123347; PMCID: PMC7095448.

5. Letko M, Marzi A, Munster V. Functional assessment of cell entry and receptor usage for SARS-CoV-2 and other lineage B betacoronaviruses. Nat Microbiol. 2020 Apr;5(4):562-569. doi: 10.1038/s41564-020-0688-y. Epub 2020 Feb 24. PMID: 32094589; PMCID: PMC7095430.

6. Shang J, Wan Y, Luo C, Ye G, Geng Q, Auerbach A, Li F. Cell entry mechanisms of SARS-CoV-2. Proc Natl Acad Sci U S A. 2020 May 26;117(21):11727-11734. doi: 10.1073/pnas.2003138117. Epub 2020 May 6. PMID: 32376634; PMCID: PMC7260975.

7. Li F. Structure, Function, and Evolution of Coronavirus Spike Proteins. Annu Rev Virol. 2016 Sep 29;3(1):237-261. doi: 10.1146/annurev-virology-110615-042301. Epub 2016 Aug 25. PMID: 27578435; PMCID: PMC5457962.

8. Turoňová B, Sikora M, Schürmann C, Hagen WJH, Welsch S, Blanc FEC, von Bülow S, Gecht M, Bagola K, Hörner C, van Zandbergen G, Landry J, de Azevedo NTD,

Mosalaganti S, Schwarz A, Covino R, Mühlebach MD, Hummer G, Krijnse Locker J, Beck M. In situ structural analysis of SARS-CoV-2 spike reveals flexibility mediated by three hinges. Science. 2020 Oct 9;370(6513):203-208. doi: 10.1126/science.abd5223. Epub 2020 Aug 18. PMID: 32817270; PMCID: PMC7665311.

9. Hoffmann M, Kleine-Weber H, Schroeder S, Krüger N, Herrler T, Erichsen S, Schiergens TS, Herrler G, Wu NH, Nitsche A, Müller MA, Drosten C, Pöhlmann S. SARS-CoV-2 Cell Entry Depends on ACE2 and TMPRSS2 and Is Blocked by a Clinically Proven Protease Inhibitor. Cell. 2020 Apr 16;181(2):271-280.e8. doi: 10.1016/j.cell.2020.02.052. Epub 2020 Mar 5. PMID: 32142651; PMCID: PMC7102627.

10. CDC, https://www.cdc.gov/coronavirus/2019-ncov/vaccines/different-vaccines.html

11. WHO, **Draft landscape and tracker of COVID-19 candidate vaccines,** https://www.who.int/publications/m/item/draft-landscape-of-covid-19-candidate-vaccines

12. Holmgren J, Czerkinsky C. Mucosal immunity and vaccines. Nat Med. 2005 Apr;11(4 Suppl):S45-53. doi: 10.1038/nm1213. PMID: 15812489.

13. Cox RJ, Brokstad KA, Ogra P. Influenza virus: immunity and vaccination strategies. Comparison of the immune response to inactivated and live, attenuated influenza vaccines. Scand J Immunol. 2004 Jan;59(1):1-15. doi: 10.1111/j.0300-9475.2004.01382.x. PMID: 14723616.

14. Sterlin D, Mathian A, Miyara M, Mohr A, Anna F, Claër L, Quentric P, Fadlallah J, Devilliers H, Ghillani P, Gunn C, Hockett R, Mudumba S, Guihot A, Luyt CE, Mayaux J, Beurton A, Fourati S, Bruel T, Schwartz O, Lacorte JM, Yssel H, Parizot C, Dorgham K, Charneau P, Amoura Z, Gorochov G. IgA dominates the early neutralizing antibody response to SARS-CoV-2. Sci Transl Med. 2021 Jan 20;13(577):eabd2223. doi: 10.1126/scitranslmed.abd2223. Epub 2020 Dec 7. PMID: 33288662; PMCID: PMC7857408.

15. See RH, Zakhartchouk AN, Petric M, Lawrence DJ, Mok CPY, Hogan RJ, Rowe T, Zitzow LA, Karunakaran KP, Hitt MM, Graham FL, Prevec L, Mahony JB, Sharon C, Auperin TC, Rini JM, Tingle AJ, Scheifele DW, Skowronski DM, Patrick DM, Voss TG, Babiuk

LA, Gauldie J, Roper RL, Brunham RC, Finlay BB. Comparative evaluation of two severe acute respiratory syndrome (SARS) vaccine candidates in mice challenged with SARS coronavirus. J Gen Virol. 2006 Mar;87(Pt 3):641-650. doi: 10.1099/vir.0.81579-0. PMID: 16476986.

16. Stobart CC, Rostad CA Ke Z, Dillard RS, Hampton CM, Strauss JD, Yi H, Hotard AL, Meng J, Pickles RJ, Sakamoto K, Lee S, Currier MG, Moin SM, Graham BS, Boukhvalova MS, Gilbert BE, Blanco JC, Piedra PA, Wright ER, Moore ML. A live RSV vaccine with engineered thermostability is immunogenic in cotton rats despite high attenuation. Nat Commun. 2016 Dec 21;7:13916. doi: 10.1038/ncomms13916. PMID: 28000669; PMCID: PMC5187593.

17. Corver J, Broer R, van Kasteren P, Spaan W. Mutagenesis of the transmembrane domain of the SARS coronavirus spike glycoprotein: refinement of the requirements for SARS coronavirus cell entry. Virol J. 2009 Dec 24;6:230. doi: 10.1186/1743-422X-6-230. PMID: 20034394; PMCID: PMC2805634.

18. Broer R, Boson B, Spaan W, Cosset FL, Corver J. Important role for the transmembrane domain of severe acute respiratory syndrome coronavirus spike protein during entry. J Virol. 2006 Feb;80(3):1302-10. doi: 10.1128/JVI.80.3.1302-1310.2006. PMID: 16415007; PMCID: PMC1346921.

19. Godeke GJ, de Haan CA, Rossen JW, Vennema H, Rottier PJ. Assembly of spikes into coronavirus particles is mediated by the carboxy-terminal domain of the spike protein. J Virol. 2000 Feb;74(3):1566-71. doi: 10.1128/jvi.74.3.1566-1571.2000. PMID: 10627571; PMCID: PMC111495.

20. Oomens AG, Bevis KP, Wertz GW. The cytoplasmic tail of the human respiratory syncytial virus F protein plays critical roles in cellular localization of the F protein and infectious progeny production. J Virol. 2006 Nov;80(21):10465-77. doi: 10.1128/JVI.01439-06. Epub 2006 Aug 23. PMID: 16928754; PMCID: PMC1641763.

21. Meng J, Lee S, Hotard AL, Moore ML. Refining the balance of attenuation and immunogenicity of respiratory syncytial virus by targeted codon deoptimization of virulence genes. mBio. 2014 Sep 23;5(5):e01704-14. doi: 10.1128/mBio.01704-14. PMID: 25249281; PMCID: PMC4173764.

22. Shcherbo D, Murphy CS, Ermakova GV, Solovieva EA, Chepurnykh TV, Shcheglov AS, Verkhusha VV, Pletnev VZ, Hazelwood KL, Roche PM, Lukyanov S, Zaraisky AG, Davidson MW, Chudakov DM. Far-red fluorescent tags for protein imaging in living tissues. Biochem J. 2009 Mar 15;418(3):567-74. doi: 10.1042/BJ20081949. PMID: 19143658; PMCID: PMC2893397.

23. Tegally H, Wilkinson E, Giovanetti M, Iranzadeh A, Fonseca V, Giandhari J, Doolabh D, Pillay S, San EJ, Msomi N, Mlisana K, von Gottberg A, Walaza S, Allam M, Ismail A, Mohale T, Glass AJ, Engelbrecht S, Van Zyl G, Preiser W, Petruccione F, Sigal A, Hardie D, Marais G, Hsiao NY, Korsman S, Davies MA, Tyers L, Mudau I, York D, Maslo C, Goedhals D, Abrahams S, Laguda-Akingba O, Alisoltani-Dehkordi A, Godzik A, Wibmer CK, Sewell BT, Lourenço J, Alcantara LCJ, Kosakovsky Pond SL, Weaver S, Martin D, Lessells RJ, Bhiman JN, Williamson C, de Oliveira T. Detection of a SARS-CoV-2 variant of concern in South Africa. Nature. 2021 Apr;592(7854):438-443. doi: 10.1038/s41586-021-03402-9. Epub 2021 Mar 9. PMID: 33690265.

24. Hotard AL, Shaikh FY, Lee S, Yan D, Teng MN, Plemper RK, Crowe JE Jr, Moore ML. A stabilized respiratory syncytial virus reverse genetics system amenable to recombination-mediated mutagenesis. Virology. 2012 Dec 5;434(1):129-36. doi: 10.1016/j.virol.2012.09.022. Epub 2012 Oct 11. PMID: 23062737; PMCID: PMC3492879.

25. Hoffmann M, Kleine-Weber H, Pöhlmann S. A Multibasic Cleavage Site in the Spike Protein of SARS-CoV-2 Is Essential for Infection of Human Lung Cells. Mol Cell. 2020 May 21;78(4):779-784.e5. doi: 10.1016/j.molcel.2020.04.022. Epub 2020 May 1. PMID: 32362314; PMCID: PMC7194065.

26. Walls AC, Park YJ, Tortorici MA, Wall A, McGuire AT, Veesler D. Structure, Function, and Antigenicity of the SARS-CoV-2 Spike Glycoprotein. Cell. 2020 Apr 16;181(2):281-292.e6. doi: 10.1016/j.cell.2020.02.058. Epub 2020 Mar 9. Erratum in: Cell. 2020 Dec 10;183(6):1735. PMID: 32155444; PMCID: PMC7102599.

27. Burkard C, Verheije MH, Wicht O, van Kasteren SI, van Kuppeveld FJ, Haagmans BL, Pelkmans L, Rottier PJ, Bosch BJ, de Haan CA. Coronavirus cell entry occurs through the endo-/lysosomal pathway in a proteolysis-dependent manner. PLoS Pathog. 2014 Nov

6;10(11):e1004502. doi: 10.1371/journal.ppat.1004502. Erratum in: PLoS Pathog. 2015 Feb;11(2):e1004709. PMID: 25375324; PMCID: PMC4223067.

28. Ou X, Liu Y, Lei X, Li P, Mi D, Ren L, Guo L, Guo R, Chen T, Hu J, Xiang Z, Mu Z, Chen X, Chen J, Hu K, Jin Q, Wang J, Qian Z. Characterization of spike glycoprotein of SARS-CoV-2 on virus entry and its immune cross-reactivity with SARS-CoV. Nat Commun. 2020 Mar 27;11(1):1620. doi: 10.1038/s41467-020-15562-9. Erratum in: Nat Commun. 2021 Apr 1;12(1):2144. PMID: 32221306; PMCID: PMC7100515.

29. Peacock TP, Goldhill DH, Zhou J, Baillon L, Frise R, Swann OC, Kugathasan R, Penn R, Brown JC, Sanchez-David RY, Braga L, Williamson MK, Hassard JA, Staller E, Hanley B, Osborn M, Giacca M, Davidson AD, Matthews DA, Barclay WS. The furin cleavage site in the SARS-CoV-2 spike protein is required for transmission in ferrets. Nat Microbiol. 2021 Apr 27. doi: 10.1038/s41564-021-00908-w. Epub ahead of print. PMID: 33907312.

30. Woolsey C, Borisevich V, Prasad AN, Agans KN, Deer DJ, Dobias NS, Heymann JC, Foster SL, Levine CB, Medina L, Melody K, Geisbert JB, Fenton KA, Geisbert TW, Cross RW. Establishment of an African green monkey model for COVID-19 and protection against re-infection. Nat Immunol. 2021 Jan;22(1):86-98. doi: 10.1038/s41590-020-00835-8. Epub 2020 Nov 24. PMID: 33235385; PMCID: PMC7790436.

31. Cross RW, Agans KN, Prasad AN, Borisevich V, Woolsey C, Deer DJ, Dobias NS, Geisbert JB, Fenton KA, Geisbert TW. Intranasal exposure of African green monkeys to SARS-CoV-2 results in acute phase pneumonia with shedding and lung injury still present in the early convalescence phase. Virol J. 2020 Aug 18;17(1):125. doi: 10.1186/s12985-020-01396-w. PMID: 32811514; PMCID: PMC7431901.

32. Blair RV, Vaccari M, Doyle-Meyers LA, Roy CJ, Russell-Lodrigue K, Fahlberg M, Monjure CJ, Beddingfield B, Plante KS, Plante JA, Weaver SC, Qin X, Midkiff CC, Lehmicke G, Golden N, Threeton B, Penney T, Allers C, Barnes MB, Pattison M, Datta PK, Maness NJ, Birnbaum A, Fischer T, Bohm RP, Rappaport J. Acute Respiratory Distress in Aged, SARS-CoV-2-Infected African Green Monkeys but Not Rhesus Macaques. Am J Pathol. 2021 Feb;191(2):274-282. doi: 10.1016/j.ajpath.2020.10.016. Epub 2020 Nov 7. PMID: 33171111; PMCID: PMC7648506.

33. Lee CY, Lowen AC. Animal models for SARS-CoV-2. Curr Opin Virol. 2021 Apr 6;48:73-81. doi: 10.1016/j.coviro.2021.03.009. Epub ahead of print. PMID: 33906125; PMCID: PMC8023231.

34. Taylor G. Animal models of respiratory syncytial virus infection. Vaccine. 2017 Jan 11;35(3):469-480. doi: 10.1016/j.vaccine.2016.11.054. Epub 2016 Nov 29. PMID: 27908639; PMCID: PMC5244256.

35. Boelen A, Andeweg A, Kwakkel J, Lokhorst W, Bestebroer T, Dormans J, Kimman T. Both immunisation with a formalin-inactivated respiratory syncytial virus (RSV) vaccine and a mock antigen vaccine induce severe lung pathology and a Th2 cytokine profile in RSV-challenged mice. Vaccine. 2000 Nov 22;19(7-8):982-91. doi: 10.1016/s0264-410x(00)00213-9. PMID: 11115725.

36. Planas D, Bruel T, Grzelak L, Guivel-Benhassine F, Staropoli I, Porrot F, Planchais C, Buchrieser J, Rajah MM, Bishop E, Albert M, Donati F, Prot M, Behillil S, Enouf V, Maquart M, Smati-Lafarge M, Varon E, Schortgen F, Yahyaoui L, Gonzalez M, De Sèze J, Péré H, Veyer D, Sève A, Simon-Lorière E, Fafi-Kremer S, Stefic K, Mouquet H, Hocqueloux L, van der Werf S, Prazuck T, Schwartz O. Sensitivity of infectious SARS-CoV-2 B.1.1.7 and B.1.351 variants to neutralizing antibodies. Nat Med. 2021 May;27(5):917-924. doi: 10.1038/s41591-021-01318-5. Epub 2021 Mar 26. PMID: 33772244.

37. Wang Z, Schmidt F, Weisblum Y, Muecksch F, Barnes CO, Finkin S, Schaefer-Babajew D, Cipolla M, Gaebler C, Lieberman JA, Oliveira TY, Yang Z, Abernathy ME, Huey-Tubman KE, Hurley A, Turroja M, West KA, Gordon K, Millard KG, Ramos V, Da Silva J, Xu J, Colbert RA, Patel R, Dizon J, Unson-O'Brien C, Shimeliovich I, Gazumyan A, Caskey M, Bjorkman PJ, Casellas R, Hatziioannou T, Bieniasz PD, Nussenzweig MC. mRNA vaccine-elicited antibodies to SARS-CoV-2 and circulating variants. Nature. 2021 Apr;592(7855):616-622. doi: 10.1038/s41586-021-03324-6. Epub 2021 Feb 10. PMID: 33567448.

38. Liu Y, Liu J, Xia H, Zhang X, Fontes-Garfias CR, Swanson KA, Cai H, Sarkar R, Chen W, Cutler M, Cooper D, Weaver SC, Muik A, Sahin U, Jansen KU, Xie X, Dormitzer PR, Shi PY. Neutralizing Activity of BNT162b2-Elicited Serum. N Engl J Med. 2021 Apr 15;384(15):1466-1468. doi: 10.1056/NEJMc2102017. Epub 2021 Mar 8. PMID: 33684280; PMCID: PMC7944950.

39. Corbett KS, Edwards DK, Leist SR, Abiona OM, Boyoglu-Barnum S, Gillespie RA, Himansu S, Schäfer A, Ziwawo CT, DiPiazza AT, Dinnon KH, Elbashir SM, Shaw CA, Woods A, Fritch EJ, Martinez DR, Bock KW, Minai M, Nagata BM, Hutchinson GB, Wu K, Henry C, Bahl K, Garcia-Dominguez D, Ma L, Renzi I, Kong WP, Schmidt SD, Wang L, Zhang Y, Phung E, Chang LA, Loomis RJ, Altaras NE, Narayanan E, Metkar M,

Presnyak V, Liu C, Louder MK, Shi W, Leung K, Yang ES, West A, Gully KL, Stevens LJ, Wang N, Wrapp D, Doria-Rose NA, Stewart-Jones G, Bennett H, Alvarado GS, Nason MC, Ruckwardt TJ, McLellan JS, Denison MR, Chappell JD, Moore IN, Morabito KM, Mascola JR, Baric RS, Carfi A, Graham BS. SARS-CoV-2 mRNA vaccine design enabled by prototype pathogen preparedness. Nature. 2020 Oct;586(7830):567-571. doi: 10.1038/s41586-020-2622-0. Epub 2020 Aug 5. PMID: 32756549; PMCID: PMC7581537.

40. Corbett KS, Flynn B, Foulds KE, Francica JR, Boyoglu-Barnum S, Werner AP, Flach B, O'Connell S, Bock KW, Minai M, Nagata BM, Andersen H, Martinez DR, Noe AT, Douek N, Donaldson MM, Nji NN, Alvarado GS, Edwards DK, Flebbe DR, Lamb E, Doria-Rose NA, Lin BC, Louder MK, O'Dell S, Schmidt SD, Phung E, Chang LA, Yap C, Todd JM, Pessaint L, Van Ry A, Browne S, Greenhouse J, Putman-Taylor T, Strasbaugh A, Campbell TA, Cook A, Dodson A, Steingrebe K, Shi W, Zhang Y, Abiona OM, Wang L, Pegu A, Yang ES, Leung K, Zhou T, Teng IT, Widge A, Gordon I, Novik L, Gillespie RA, Loomis RJ, Moliva JI, Stewart-Jones G, Himansu S, Kong WP, Nason MC, Morabito KM, Ruckwardt TJ, Ledgerwood JE, Gaudinski MR, Kwong PD, Mascola JR, Carfi A, Lewis MG, Baric RS, McDermott A, Moore IN, Sullivan NJ, Roederer M, Seder RA, Graham BS. Evaluation of the mRNA-1273 Vaccine against SARS-CoV-2 in Nonhuman Primates. N Engl J Med. 2020 Oct 15;383(16):1544-1555. doi: 10.1056/NEJMoa2024671. Epub 2020 Jul 28. PMID: 32722908; PMCID: PMC7449230.

41. Guebre-Xabier M, Patel N, Tian JH, Zhou B, Maciejewski S, Lam K, Portnoff AD, Massare MJ, Frieman MB, Piedra PA, Ellingsworth L, Glenn G, Smith G. NVX-CoV2373 vaccine protects cynomolgus macaque upper and lower airways against SARS-CoV-2 challenge. Vaccine. 2020 Nov 25;38(50):7892-7896. doi: 10.1016/j.vaccine.2020.10.064. Epub 2020 Oct 23. PMID: 33139139; PMCID: PMC7584426.

42. van der Fits L, Bolder R, Heemskerk-van der Meer M, Drijver J, van Polanen Y, Serroyen J, Langedijk JPM, Schuitemaker H, Saeland E, Zahn R. Adenovector 26 encoded prefusion conformation stabilized RSV-F protein induces long-lasting Th1-biased immunity in neonatal mice. NPJ Vaccines. 2020 Jun 12;5(1):49. doi: 10.1038/s41541-020-0200-y. PMID: 33580084.

43. Yahalom-Ronen Y, Tamir H, Melamed S, Politi B, Shifman O, Achdout H, Vitner EB, Israeli O, Milrot E, Stein D, Cohen-Gihon I, Lazar S, Gutman H, Glinert I, Cherry L, Vagima Y, Lazar S, Weiss S, Ben-Shmuel A, Avraham R, Puni R, Lupu E, Bar-David E, Sittner A, Erez N, Zichel R, Mamroud E, Mazor O, Levy H, Laskar O, Yitzhaki S, Shapira SC, Zvi A, Beth-Din A, Paran N, Israely T. A single dose of recombinant VSV-ΔG-spike vaccine provides protection against SARS-CoV-2 challenge. Nat Commun. 2020 Dec

16;11(1):6402. doi: 10.1038/s41467-020-20228-7. PMID: 33328475; PMCID: PMC7745033.

44. Case JB, Rothlauf PW, Chen RE, Liu Z, Zhao H, Kim AS, Bloyet LM, Zeng Q, Tahan S, Droit L, Ilagan MXG, Tartell MA, Amarasinghe G, Henderson JP, Miersch S, Ustav M, Sidhu S, Virgin HW, Wang D, Ding S, Corti D, Theel ES, Fremont DH, Diamond MS, Whelan SPJ. Neutralizing Antibody and Soluble ACE2 Inhibition of a Replication-Competent VSV-SARS-CoV-2 and a Clinical Isolate of SARS-CoV-2. Cell Host Microbe. 2020 Sep 9;28(3):475-485.e5. doi: 10.1016/j.chom.2020.06.021. Epub 2020 Jul 3. PMID: 32735849; PMCID: PMC7332453

45. Dieterle ME, Haslwanter D, Bortz RH 3rd, Wirchnianski AS, Lasso G, Vergnolle O, Abbasi SA, Fels JM, Laudermilch E, Florez C, Mengotto A, Kimmel D, Malonis RJ, Georgiev G, Quiroz J, Barnhill J, Pirofski LA, Daily JP, Dye JM, Lai JR, Herbert AS, Chandran K, Jangra RK. A Replication-Competent Vesicular Stomatitis Virus for Studies of SARS-CoV-2spike-Mediated Cell Entry and Its Inhibition. Cell Host Microbe. 2020 Sep 9;28(3):486-496.e6. doi: 10.1016/j.chom.2020.06.020. Epub 2020 Jul 3. PMID: 32738193; PMCID: PMC7332447.

46. Vogel AB, Kanevsky I, Che Y, Swanson KA, Muik A, Vormehr M, Kranz LM, Walzer KC, Hein S, Güler A, Loschko J, Maddur MS, Ota-Setlik A, Tompkins K, Cole J, Lui BG, Ziegenhals T, Plaschke A, Eisel D, Dany SC, Fesser S, Erbar S, Bates F, Schneider D, Jesionek B, Sänger B, Wallisch AK, Feuchter Y, Junginger H, Krumm SA, Heinen AP, Adams-Quack P, Schlereth J, Schille S, Kröner C, de la Caridad Güimil Garcia R, Hiller T, Fischer L, Sellers RS, Choudhary S, Gonzalez O, Vascotto F, Gutman MR, Fontenot JA, Hall-Ursone S, Brasky K, Griffor MC, Han S, Su AAH, Lees JA, Nedoma NL, Mashalidis EH, Sahasrabudhe PV, Tan CY, Pavliakova D, Singh G, Fontes-Garfias C, Pride M, Scully IL, Ciolino T, Obregon J, Gazi M, Carrion R Jr, Alfson KJ, Kalina WV, Kaushal D, Shi PY, Klamp T, Rosenbaum C, Kuhn AN, Türeci Ö, Dormitzer PR, Jansen KU, Sahin U. BNT162b vaccines protect rhesus macaques from SARS-CoV-2. Nature. 2021 Apr;592(7853):283-289. doi: 10.1038/s41586-021-03275-y. Epub 2021 Feb 1. PMID: 33524990.

47. Mercado NB, Zahn R, Wegmann F, Loos C, Chandrashekar A, Yu J, Liu J, Peter L, McMahan K, Tostanoski LH, He X, Martinez DR, Rutten L, Bos R, van Manen D, Vellinga J, Custers J, Langedijk JP, Kwaks T, Bakkers MJG, Zuijdgeest D, Rosendahl Huber SK, Atyeo C, Fischinger S, Burke JS, Feldman J, Hauser BM, Caradonna TM, Bondzie EA, Dagotto G, Gebre MS, Hoffman E, Jacob-Dolan C, Kirilova M, Li Z, Lin Z, Mahrokhian SH, Maxfield LF, Nampanya F, Nityanandam R, Nkolola JP, Patel S, Ventura JD, Verrington K, Wan H, Pessaint L, Van Ry A, Blade K, Strasbaugh A, Cabus M, Brown R, Cook A, Zouantchangadou S, Teow E, Andersen H, Lewis MG, Cai Y, Chen B, Schmidt

AG, Reeves RK, Baric RS, Lauffenburger DA, Alter G, Stoffels P, Mammen M, Van Hoof J, Schuitemaker H, Barouch DH. Single-shot Ad26 vaccine protects against SARS-CoV-2 in rhesus macaques. Nature. 2020 Oct;586(7830):583-588. doi: 10.1038/s41586-020-2607-z. Epub 2020 Jul 30. Erratum in: Nature. 2021 Feb;590(7844):E25. PMID: 32731257; PMCID: PMC7581548.

48. van Doremalen N, Lambe T, Spencer A, Belij-Rammerstorfer S, Purushotham JN, Port JR, Avanzato VA, Bushmaker T, Flaxman A, Ulaszewska M, Feldmann F, Allen ER, Sharpe H, Schulz J, Holbrook M, Okumura A, Meade-White K, Pérez-Pérez L, Edwards NJ, Wright D, Bissett C, Gilbride C, Williamson BN, Rosenke R, Long D, Ishwarbhai A, Kailath R, Rose L, Morris S, Powers C, Lovaglio J, Hanley PW, Scott D, Saturday G, de Wit E, Gilbert SC, Munster VJ. ChAdOx1 nCoV-19 vaccine prevents SARS-CoV-2 pneumonia in rhesus macaques. Nature. 2020 Oct;586(7830):578-582. doi: 10.1038/s41586-020-2608-y. Epub 2020 Jul 30. Erratum in: Nature. 2021 Feb;590(7844):E24. PMID: 32731258.

49. Habibi MS, Jozwik A, Makris S, Dunning J, Paras A, DeVincenzo JP, de Haan CA, Wrammert J, Openshaw PJ, Chiu C; Mechanisms of Severe Acute Influenza Consortium Investigators. Impaired Antibody-mediated Protection and Defective IgA B-Cell Memory in Experimental Infection of Adults with Respiratory Syncytial Virus. Am J Respir Crit Care Med. 2015 May 1;191(9):1040-9. doi: 10.1164/rccm.201412-2256OC. PMID: 25730467; PMCID: PMC4435460.

50. Wang Z, Lorenzi JCC, Muecksch F, Finkin S, Viant C, Gaebler C, Cipolla M, Hoffmann HH, Oliveira TY, Oren DA, Ramos V, Nogueira L, Michailidis E, Robbiani DF, Gazumyan A, Rice CM, Hatziioannou T, Bieniasz PD, Caskey M, Nussenzweig MC. Enhanced SARS-CoV-2 neutralization by dimeric IgA. Sci Transl Med. 2021 Jan 20;13(577):eabf1555. doi: 10.1126/scitranslmed.abf1555. Epub 2020 Dec 7. PMID: 33288661; PMCID: PMC7857415.

51. Sterlin D, Mathian A, Miyara M, Mohr A, Anna F, Claër L, Quentric P, Fadlallah J, Devilliers H, Ghillani P, Gunn C, Hockett R, Mudumba S, Guihot A, Luyt CE, Mayaux J, Beurton A, Fourati S, Bruel T, Schwartz O, Lacorte JM, Yssel H, Parizot C, Dorgham K, Charneau P, Amoura Z, Gorochov G. IgA dominates the early neutralizing antibody response to SARS-CoV-2. Sci Transl Med. 2021 Jan 20;13(577):eabd2223. doi: 10.1126/scitranslmed.abd2223. Epub 2020 Dec 7. PMID: 33288662; PMCID: PMC7857408.

52. McDonald SM, Nelson MI, Turner PE, Patton JT. Reassortment in segmented RNA viruses: mechanisms and outcomes. Nat Rev Microbiol. 2016 Jul;14(7):448-60. doi: 10.1038/nrmicro.2016.46. Epub 2016 May 23. PMID: 27211789; PMCID: PMC5119462.

53. Spann KM, Collins PL, Teng MN. Genetic recombination during coinfection of two mutants of human respiratory syncytial virus. J Virol. 2003 Oct;77(20):11201-11. doi: 10.1128/jvi.77.20.11201-11211.2003. PMID: 14512568; PMCID: PMC224979.

54. Han GZ, Worobey M. Homologous recombination in negative sense RNA viruses. Viruses. 2011 Aug;3(8):1358-73. doi: 10.3390/v3081358. Epub 2011 Aug 4. PMID: 21994784; PMCID: PMC3185808.

55. Tan L, Lemey P, Houspie L, Viveen MC, Jansen NJ, van Loon AM, Wiertz E, van Bleek GM, Martin DP, Coenjaerts FE. Genetic variability among complete human respiratory syncytial virus subgroup A genomes: bridging molecular evolutionary dynamics and epidemiology. PLoS One. 2012;7(12):e51439. doi: 10.1371/journal.pone.0051439. Epub 2012 Dec 7. PMID: 23236501; PMCID: PMC3517519.

56. Rostad CA, Stobart CC, Todd SO, Molina SA, Lee S, Blanco JCG, Moore ML. Enhancing the Thermostability and Immunogenicity of a Respiratory Syncytial Virus (RSV) Live-Attenuated Vaccine by Incorporating Unique RSV Line19F Protein Residues. J Virol. 2018 Feb 26;92(6):e01568-17. doi: 10.1128/JVI.01568-17. PMID: 29263264; PMCID: PMC5827408.

57. Rostad CA, Stobart CC, Gilbert BE, Pickles RJ, Hotard AL, Meng J, Blanco JCG, Moin SM, Graham BS, Piedra PA, Moore ML. A Recombinant Respiratory Syncytial Virus Vaccine Candidate Attenuated by a Low-Fusion F Protein Is Immunogenic and Protective against Challenge in Cotton Rats. J Virol. 2016 Jul 27;90(16):7508-7518. doi: 10.1128/JVI.00012-16. PMID: 27279612; PMCID: PMC4984630.

58. Cheng X, Zhou H, Tang RS, Munoz MG, Jin H. Chimeric subgroup A respiratory syncytial virus with the glycoproteins substituted by those of subgroup B and RSV without the M2-2 gene are attenuated in African green monkeys. Virology. 2001 Apr 25;283(1):59-68. doi: 10.1006/viro.2001.0894. PMID: 11312662.

59. Jin H, Cheng X, Traina-Dorge VL, Park HJ, Zhou H, Soike K, Kemble G. Evaluation of recombinant respiratory syncytial virus gene deletion mutants in African green monkeys

for their potential as live attenuated vaccine candidates. Vaccine. 2003 Sep 8;21(25-26):3647-52. doi: 10.1016/s0264-410 (03)00426-2. PMID: 12922094.

60. Tang RS, MacPhail M, Schickli JH, Kaur J, Robinson CL, Lawlor HA, Guzzetta JM, Spaete RR, Haller AA. Parainfluenza virus type 3 expressing the native or soluble fusion (F) Protein of Respiratory Syncytial Virus (RSV) confers protection from RSV infection in African green monkeys. J Virol. 2004 Oct;78(20):11198-207. doi: 10.1128/JVI.78.20.11198-11207.2004. PMID: 15452239; PMCID: PMC521851.

61. Le Nouën C, Brock LG, Luongo C, McCarty T, Yang L, Mehedi M, Wimmer E, Mueller S, Collins PL, Buchholz UJ, DiNapoli JM. Attenuation of human respiratory syncytial virus by genome-scale codon-pair deoptimization. Proc Natl Acad Sci U S A. 2014 Sep 9;111(36):13169-74. doi: 10.1073/pnas.1411290111. Epub 2014 Aug 25. PMID: 25157129; PMCID: PMC4246931.

62. Hassan AO, Kafai NM, Dmitriev IP, Fox JM, Smith BK, Harvey IB, Chen RE, Winkler ES, Wessel AW, Case JB, Kashentseva E, McCune BT, Bailey AL, Zhao H, VanBlargan LA, Dai YN, Ma M, Adams LJ, Shrihari S, Danis JE, Gralinski LE, Hou YJ, Schäfer A, Kim AS, Keeler SP, Weiskopf D, Baric RS, Holtzman MJ, Fremont DH, Curiel DT, Diamond MS. A Single-Dose Intranasal ChAd Vaccine Protects Upper and Lower Respiratory Tracts against SARS-CoV-2. Cell. 2020 Oct 1;183(1):169-184.e13. doi: 10.1016/j.cell.2020.08.026. Epub 2020 Aug 19. PMID: 32931734; PMCID: PMC7437481.

63. Muruato AE, Fontes-Garfias CR, Ren P, Garcia-Blanco MA, Menachery VD, Xie X, Shi PY. A high-throughput neutralizing antibody assay for COVID-19 diagnosis and vaccine evaluation. Nat Commun. 2020 Aug 13;11(1):4059. doi: 10.1038/s41467-020-17892-0. PMID: 32792628; PMCID: PMC7426916.

64. Xie X, Muruato A, Lokugamage KG, Narayanan K, Zhang X, Zou J, Liu J, Schindewolf C, Bopp NE, Aguilar PV, Plante KS, Weaver SC, Makino S, LeDuc JW, Menachery VD, Shi PY. An Infectious cDNA Clone of SARS-CoV-2. Cell Host Microbe. 2020 May 13;27(5):841-848.e3. doi: 10.1016/j.chom.2020.04.004. Epub 2020 Apr 13. PMID: 32289263; PMCID: PMC7153529.

65. Tiboni M, Casettari L, Illum L. Nasal vaccination against SARS-CoV-2: Synergistic or alternative to intramuscular vaccines? Int J Pharm. 2021 Jun 15;603:120686. doi: 10.1016/j.ijpharm.2021.120686. Epub 2021 May 6. PMID: 33964339; PMCID: PMC8099545.

66. Press Release from Altimmune, https://ir.altimmune.com/news-releases/news-release-details/altimmune-announces-update-adcovidtm-phase-1-clinical-trial.

Figure Legends

Figure 1. Design of MV-014-212. In MV-014-212, the NS1 and NS2 genes are deoptimized and the RSV SH, G and F genes are deleted and replaced by a gene encoding a chimeric protein spike-F. The amino acid sequence at the junction is shown below the block graphic. The transmembrane domain of spike is represented in green, and the cytoplasmic tail of F is depicted in blue. The reporter virus MVK-014-212, encoding the fluorescent protein mKate2 in the first gene position, is schematically shown at the bottom or the panel.
NTD: N-terminal domain. RBD: Receptor binding domain. S1: subunit S1. S2: Subunit S2. S1/S2 and S2': protease cleavage sites. FP: fusion peptide. IFP: Internal fusion peptide. HR1 and 2: heptad repeats 1 and 2. TM: transmembrane domain. CT: cytoplasmic tail.

Figure 2: A. Syncytia formed by MV-014-212 and MVK-014-212. Micrographs were taken at a total amplification of 100X under phase contrast or using TRITC filter. Yellow arrows point to syncytia. **B. Western blot** showing full-length purified SARS-CoV-2 spike protein lacking the furin cleavage site (LakePharma, lane 1), MVK-014-212 (lane 2), MV-014-212 (lane 3), mock-infected Vero cell lysate (lane 4), blank, (water, lane 5). The molecular weight marks correspond to the migration of the BIO-RAD Precision Plus Protein Dual Color Standards. The blue arrows indicate the expected migration of the full-length spike and the cleaved protein (S1+S2). **C. Multicycle replication kinetics of MV-014-212 compared to RSV A2** in serum-free Vero cells. Cells were infected at an MOI of 0.01 and incubated at 32°C. Cells and supernatants were collected at 0, 12, 24, 48, 72, 96, and 120 hours post-infection. Titers of the samples were determined by plaque assay in Vero cells. Data points represent the means of two replicate wells and error bars represent the standard deviation. **D. Multicycle replication kinetics of MV-014-212 compared with MVK-014-212** in serum-free Vero cells. Cells were infected at an MOI of 0.01 and incubated at 32°C. Cells and supernatants were collected at 0, 3, 24, and 72 hours post-infection. Titers of the samples were determined by plaque assay in Vero cells. Data points represent the means of three replicate wells and error bars represent the standard deviation. **E. Short-term thermal stability assay**. Virus stocks of MV-014-212 prepared in Williams E medium supplemented with Sucrose Phosphate Glutamate Buffer (SPG) or prepared in SPG alone were incubated for 6 hr at -80ºC, 4ºC, -20ºC and room temperature and the titer after incubation was determined by plaque assay.

Figure 3 A. AGM study design. Nasal swabs (NS) were obtained on Days 1 through 12. Bronchoalveolar lavage (BAL) were collected on Days 2, 4, 6, 8, 10 and 12. Viral shedding in NS and BAL samples were determined by plaque assay using fresh samples. On Day 28 post-inoculation AGMs were challenged with *wt* SARS-CoV-2. Nasal swabs were obtained every day from Day 29 through 38. Bronchoalveolar lavage was obtained on alternate days starting on Day 30 to Day 38. RT-qPCR was used for detecting SARS-CoV-2 shedding in NS and BAL samples. **B. Attenuation of MV-014-212 in the upper and lower respiratory tract of AGM.** Viral titer

in nasal swabs (A) or BAL (B) from AGMs following inoculation with MV-014-212 or *wt* RSV A2 were measured by plaque assay on Vero cells. On Days 1 through 12 post-inoculation nasal swabs were collected in Williams E supplemented with SPG. Viral titer in BAL were measured on Days 2, 4, 6, 8, 10, and 12 post-inoculation. The horizontal line in the box is the mean value of the data points for each time point. The dotted line represents the LOD (50 PFU/mL). For shedding kinetics of individual animals see Fig. S5. **C. Protection of MV-014-212 vaccinated AGMs against wt SARS-CoV-2 challenge (sgRNA).** *w*t SARS-CoV-2 sgRNA in nasal swab samples from AGMs inoculated with MV-014-212, *wt* RSV A2 or PBS (Mock) following challenge. At Day 28, animals were challenged with 1.0 x 10^6 $TCID_{50}$ of *wt* SARS-CoV-2 by intranasal and intratracheal inoculation. Nasal swabs collected on Days 1, 2, 4, and 6 post-challenge with *wt* SARS-CoV-2 were shown. The level of SARS-CoV-2 sgRNA was determined by RT-qPCR. The dashed line represents the LOD of 50 genome equivalents (GE)/mL. For shedding kinetics of individual animals see Fig. S6.

Figure 4 Spike-specific antibody responses in MV-014-212 inoculated AGMs. A. Spike-specific serum IgG Antibodies specific to SARS-CoV-2 spike protein were measured by ELISA using serum collected on Day 25 from AGM inoculated with MV-014-212, *wt* RSV A2, or PBS (mock). The titer is expressed as ELISA units (ELU) / mL that were calculated by comparison to a standard curve generated from pooled human convalescent serum. **B. Spike-specific mucosal IgA.** IgA antibodies specific to SARS-CoV-2 spike protein were measured by ELISA using nasal swabs collected on Day 25 post inoculation. The Log2 of the ratio of the values obtained at day 25 over day 1 are shown. The calculated ELU/mL concentration was obtained from a standard curve generated from total purified human IgA using a capture ELISA.

Statistical analysis was one-way ANOVA. **$p<0.01$

Figure 5 Neutralization Assays with AGM sera.

A. Representative microneutralization assay performed with the fluorescent reporter virus MVK-014-212. The top two rows are the cell-only and virus-only controls. The third row corresponds to the serum of an AGM immunized with MV-014-212 (AGM #1). The numbers on top represent the serum dilutions used and the number below each well is the count of viral plaques (that appear as red foci in the wells). The image of each well was captured with a Celigo Image Cytometer (Nexcelom) and the Celigo proprietary software was used to count the plaques. **B. Microneutralization assay using MVK-014-212.** Neutralizing titers (NT50) in serum of AGMs immunized either with MV-014-212 or the negative controls, RSV or Mock, obtained from a microneutralization assay (performed as in A). The plaque count from A was used to calculate the NT50 as described in Methods. **C. Microneutralization assay using MVK-014-212** comparing the NT50 of two AGM immunized with MV-014-212 to a convalescent control at 1859 IU/mL.

The two animals used in this experiment correspond to the animals with highest titers in experiment B. **D. Plaque Reduction Neutralization Assay.** Serum from AGM#1 immunized with MV-014-212 was used in a 50% plaque-reduction neutralization test performed in a BSL-3 facility (Muruato 2020, Liu 2021). The neutralization titers of AGM#1 against *wt* SARS-CoV-2 or two variants of concern (B.1.351 and B.1.1.7) are shown. The convalescent serum ("Conv.") used in this assay is the same as in C. LOD is 20 and is indicated as a dashed line.

In all cases, the data shown is the average of two technical replicates. Statistical analysis was one-way ANOVA. *$p<0.05$

Figure 6 MV-014-212 elicited a Th1-biased immune response in ACE-2 mice. A. ELISpot: IFNγ (left) or IL-5 (right) producing cells in ACE-2 mice. Splenocytes isolated from hACE-2 expressing mice (n=5) were collected on Day 28 post-inoculation (with MV-014-212 or PBS) and stimulated with a peptide pool that spanned the SARS-CoV-2 spike protein (pool), media, or the mitogen concanavalin A (Con A). IL-5 or IFN-γ expressing T-cells were quantified by ELISpot assay. Control mice were vaccinated with purified SARS-CoV-2 spike protein adjuvanted with alum by intramuscular injection at Day -20 and Day 0. **B.** Logarithm of the ratio of IFN-γ to IL-5 expressing cells (as shown in A.) **C**. **IgG1 and IgG2a ELISA.** Levels of IgG2a (left panel) and IgG1 (right panel) corresponding to Day 28 serum from hACE-2 mice vaccinated intranasally with PBS or MV-014-212 or intramuscularly with spike-alum, as determined by ELISA. The concentration of each immunoglobulin isotype was determined from standard curves generated with purified SARS-CoV-2 spike specific monoclonal IgG2a or IgG1 antibodies. **D.** Logarithm of the ratio of IgG2a/IgG1 (as shown in C). Statistical analysis is an unpaired t-test. ****$P<0.0001$

Figure 1

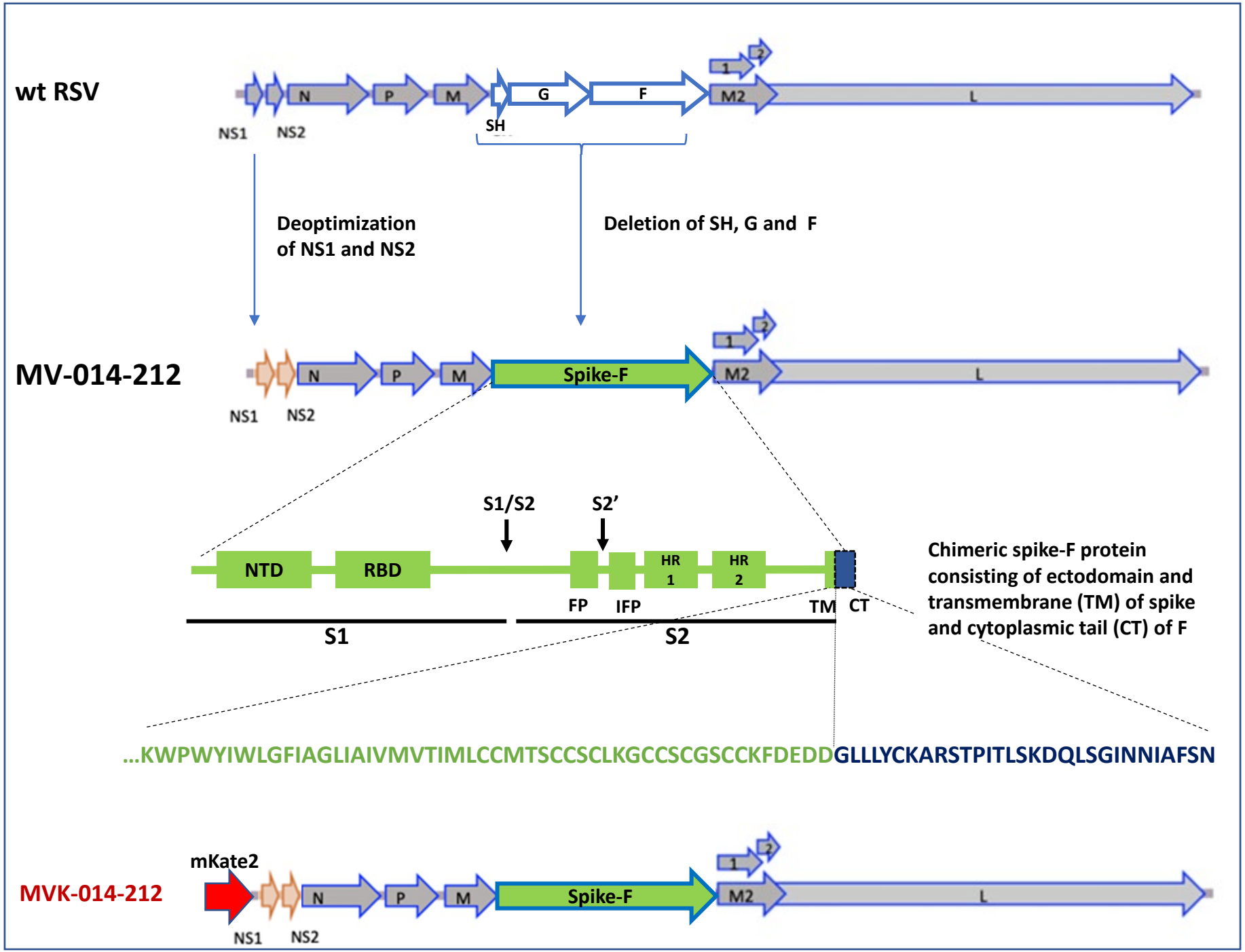
wt RSV
NS1
NS2
N
P
M
SH
G
F
1
2
M2
L
Deoptimization of NS1 and NS2
Deletion of SH, G and F
MV-014-212
Spike-F
S1/S2
S2'
NTD
RBD
HR 1
HR 2
FP
IFP
TM
CT
S1
S2
Chimeric spike-F protein consisting of ectodomain and transmembrane (TM) of spike and cytoplasmic tail (CT) of F
...KWPWYIWLGFIAGLIAIVMVTIMLCCMTSCCSCLKGCCSCGSCCKFDEDDGLLLYCKARSTPITLSKDQLSGINNIAFSN
MVK-014-212
mKate2

Figure 2

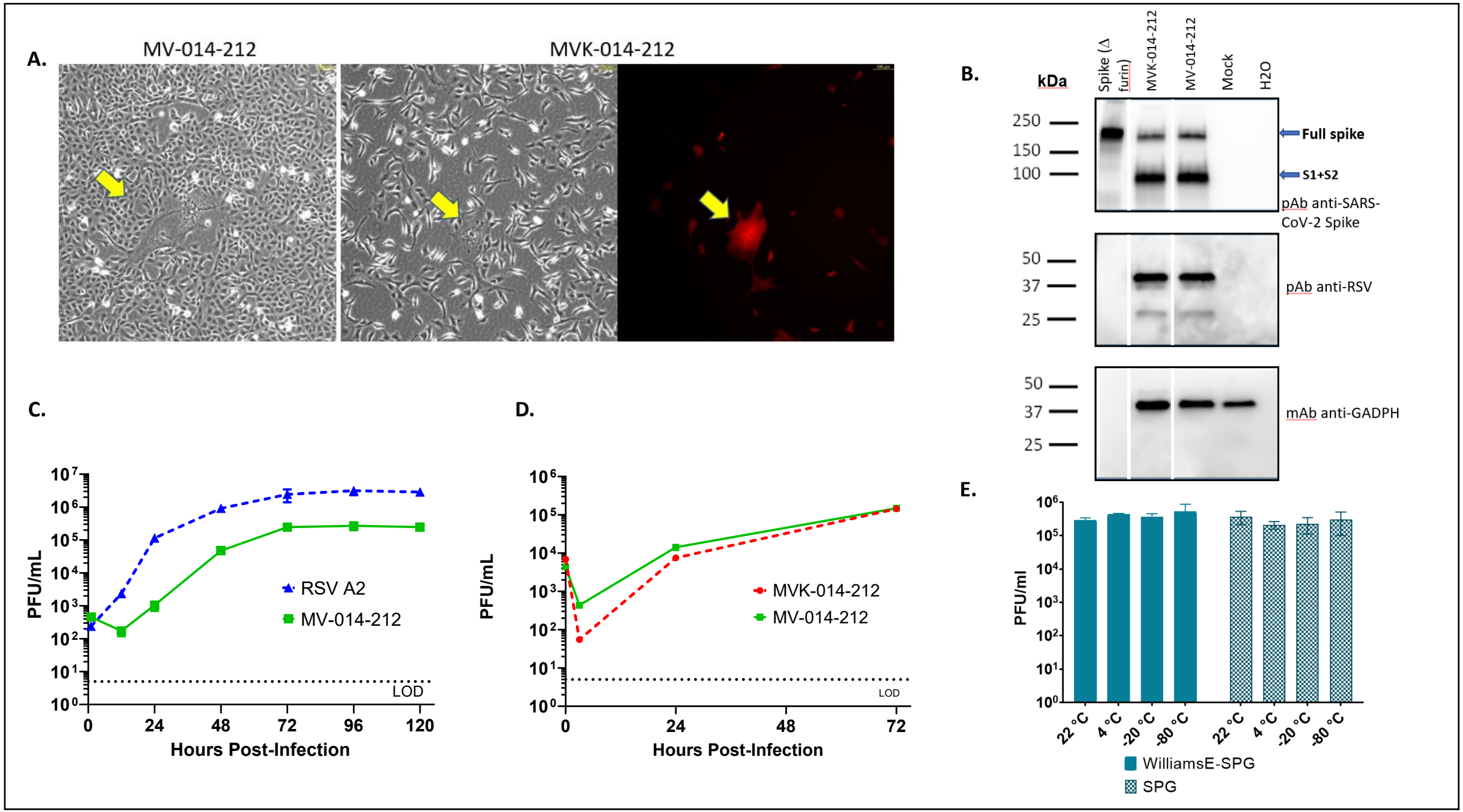
A.
MV-014-212
MVK-014-212
B.
kDa
Spike (Δ furin)
MVK-014-212
MV-014-212
Mock
H2O
250
150
100
Full spike
S1+S2
pAb anti-SARS-CoV-2 Spike
50
37
25
pAb anti-RSV
50
37
25
mAb anti-GADPH
C.
PFU/mL
RSV A2
MV-014-212
LOD
Hours Post-Infection
D.
PFU/mL
MVK-014-212
MV-014-212
LOD
Hours Post-Infection
E.
PFU/ml
22 °C
4 °C
-20 °C
-80 °C
WilliamsE-SPG
SPG

Figure 3A

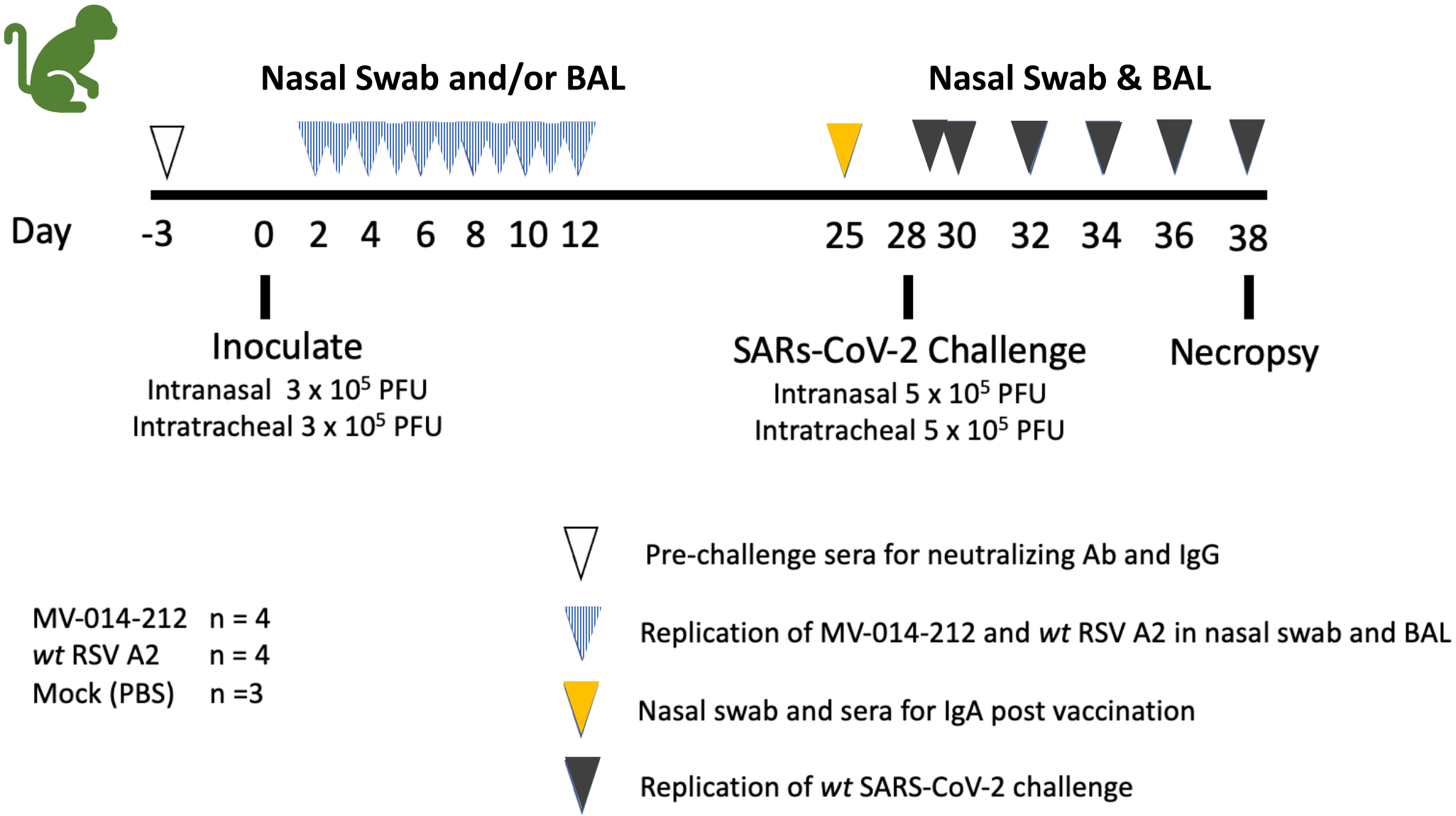
Nasal Swab and/or BAL
Nasal Swab & BAL
Day
-3
0
2
4
6
8
10
12
25
28
30
32
34
36
38
Inoculate
Intranasal 3 x 10^5 PFU
Intratracheal 3 x 10^5 PFU
SARs-CoV-2 Challenge
Intranasal 5 x 10^5 PFU
Intratracheal 5 x 10^5 PFU
Necropsy
MV-014-212 n = 4
wt RSV A2 n = 4
Mock (PBS) n =3
Pre-challenge sera for neutralizing Ab and IgG
Replication of MV-014-212 and wt RSV A2 in nasal swab and BAL
Nasal swab and sera for IgA post vaccination
Replication of wt SARS-CoV-2 challenge

Figure 3B

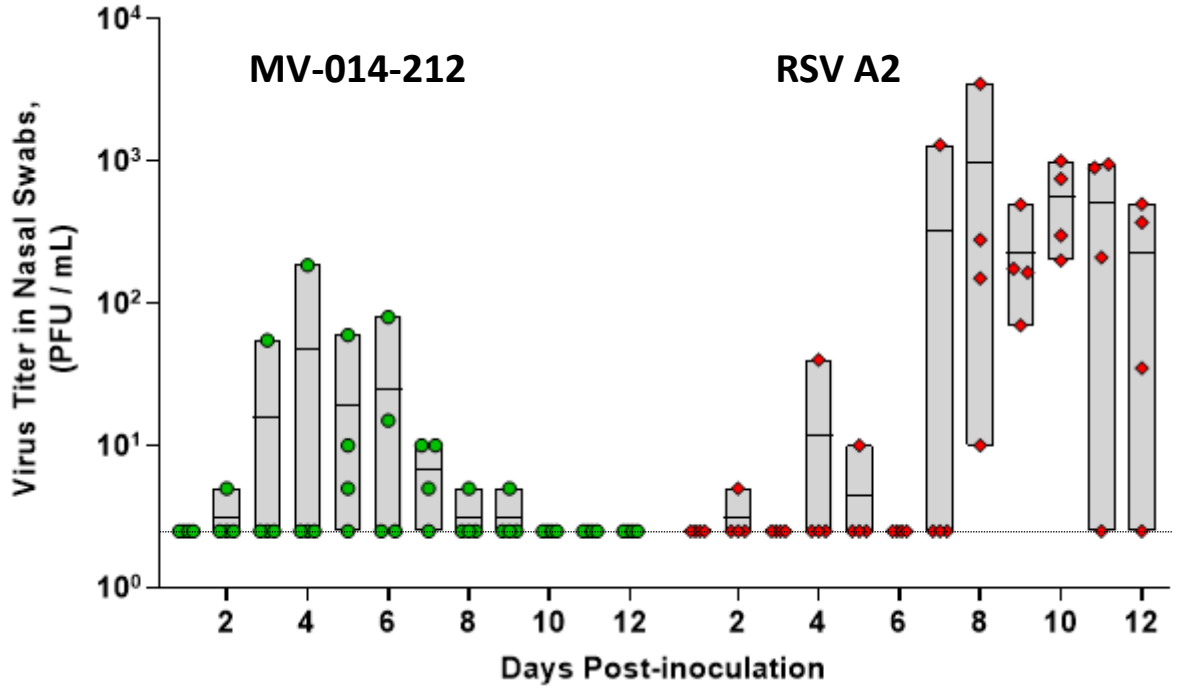
MV-014-212
RSV A2
Virus Titer in Nasal Swabs, (PFU / mL)
10^4
10^3
10^2
10^1
10^0
2 4 6 8 10 12 2 4 6 8 10 12
Days Post-inoculation

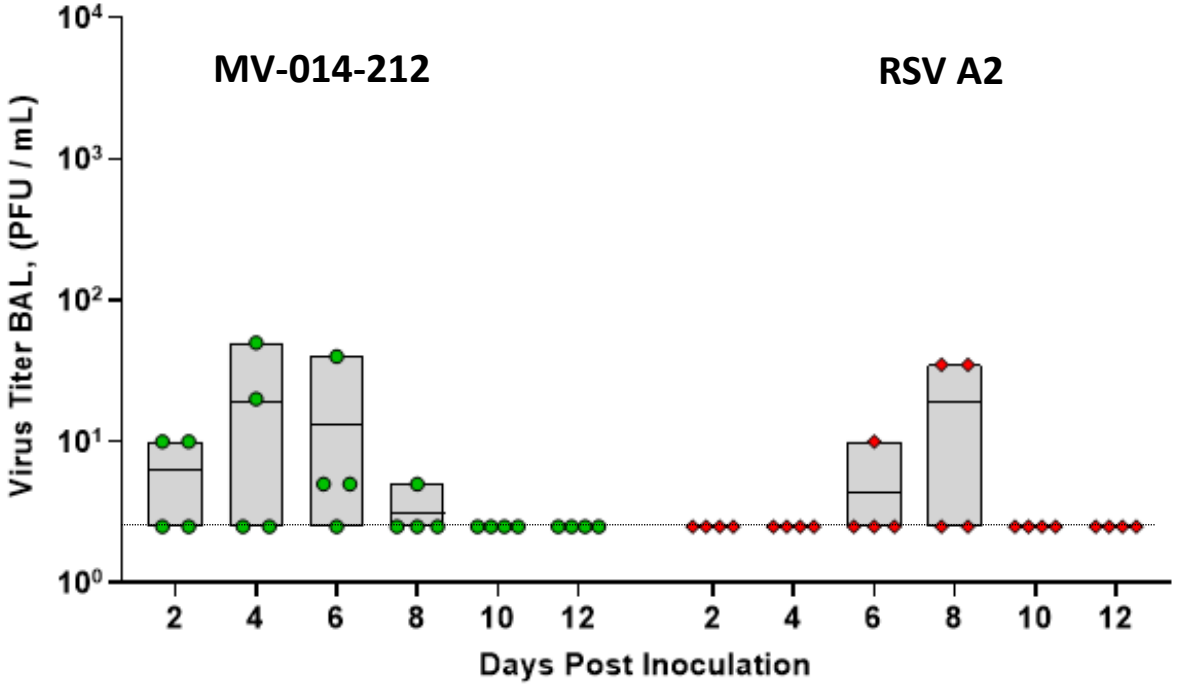
MV-014-212
RSV A2
Virus Titer BAL, (PFU / mL)
10^4
10^3
10^2
10^1
10^0
2 4 6 8 10 12 2 4 6 8 10 12
Days Post Inoculation

Figure 3C

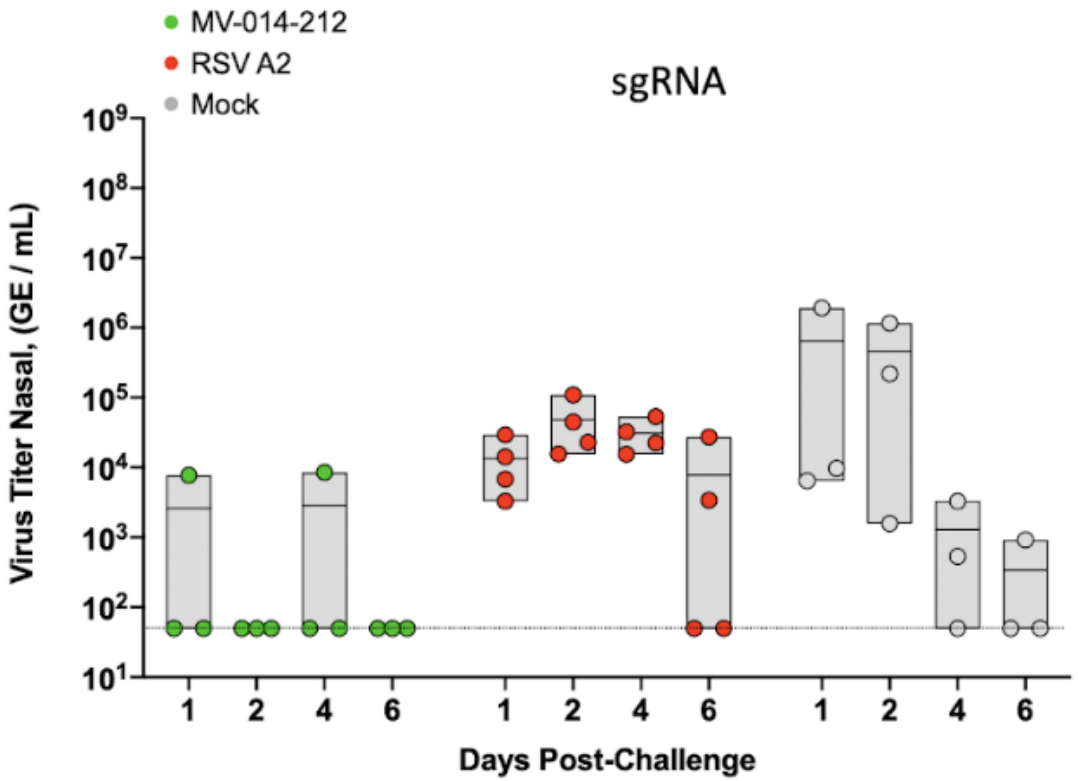
MV-014-212
RSV A2
Mock
sgRNA
Virus Titer Nasal, (GE / mL)
10^9
10^8
10^7
10^6
10^5
10^4
10^3
10^2
10^1
1 2 4 6 1 2 4 6 1 2 4 6
Days Post-Challenge

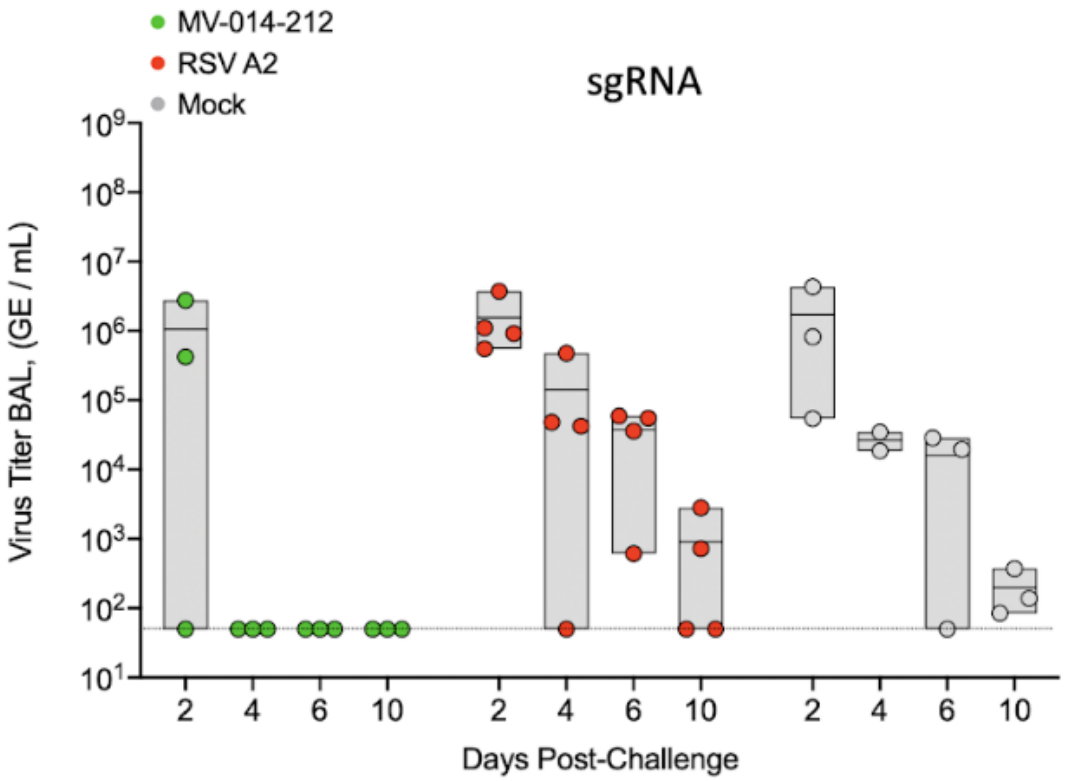
MV-014-212
RSV A2
Mock
sgRNA
Virus Titer BAL, (GE / mL)
10^9
10^8
10^7
10^6
10^5
10^4
10^3
10^2
10^1
2 4 6 10 2 4 6 10 2 4 6 10
Days Post-Challenge

Figure 4

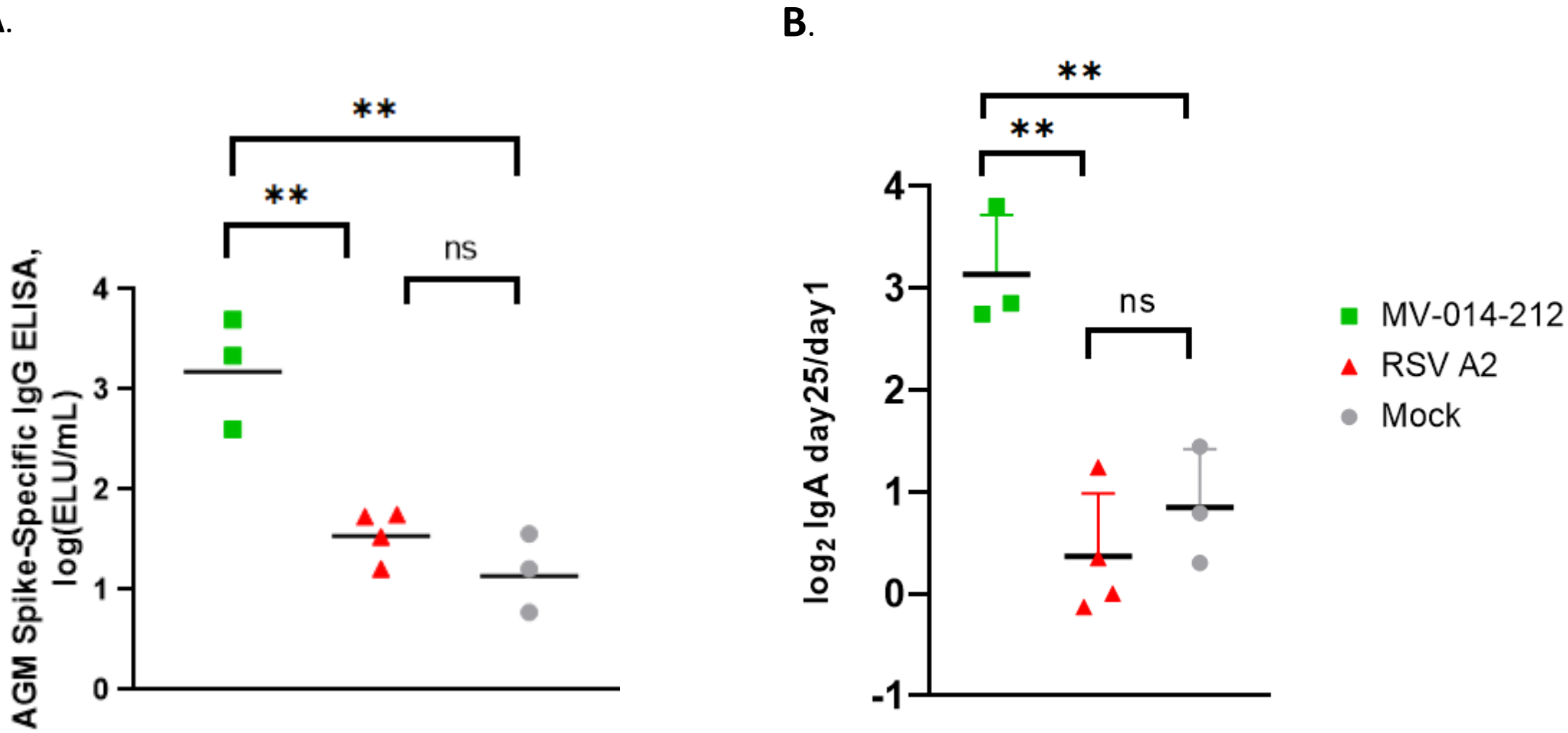
A.
**
**
ns
AGM Spike-Specific IgG ELISA, log(ELU/mL)
4
3
2
1
0
B.
**
**
ns
log_2 IgA day25/day1
4
3
2
1
0
-1
MV-014-212
RSV A2
Mock

Figure 5

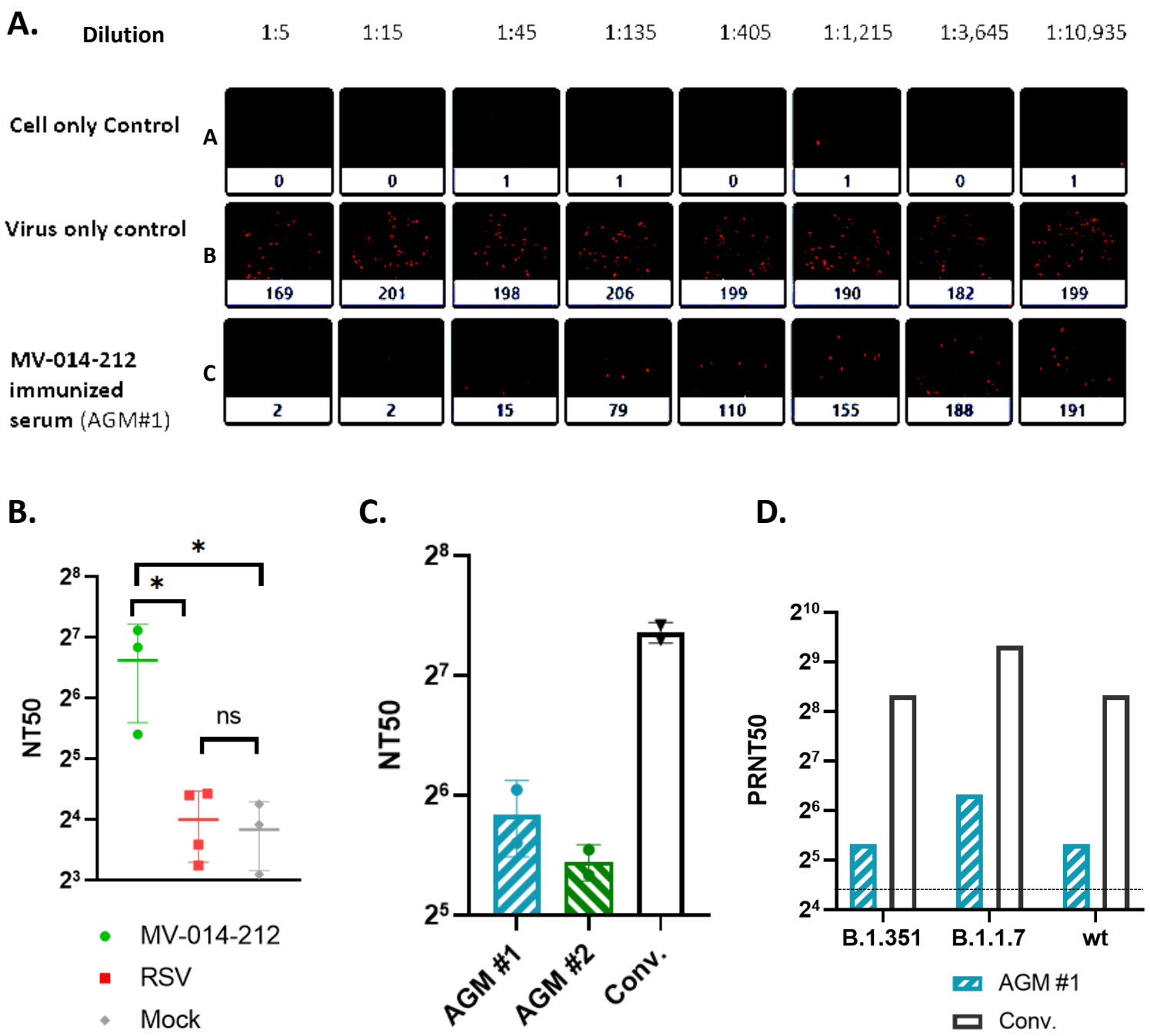
A.
Dilution
1:5
1:15
1:45
1:135
1:405
1:1,215
1:3,645
1:10,935
Cell only Control
A
0
0
1
1
0
1
0
1
Virus only control
B
169
201
198
206
199
190
182
199
MV-014-212 immunized serum (AGM#1)
C
2
2
15
79
110
155
188
191
B.
NT50
ns
MV-014-212
RSV
Mock
C.
NT50
AGM #1
AGM #2
Conv.
D.
PRNT50
B.1.351
B.1.1.7
wt
AGM #1
Conv.

Figure 6

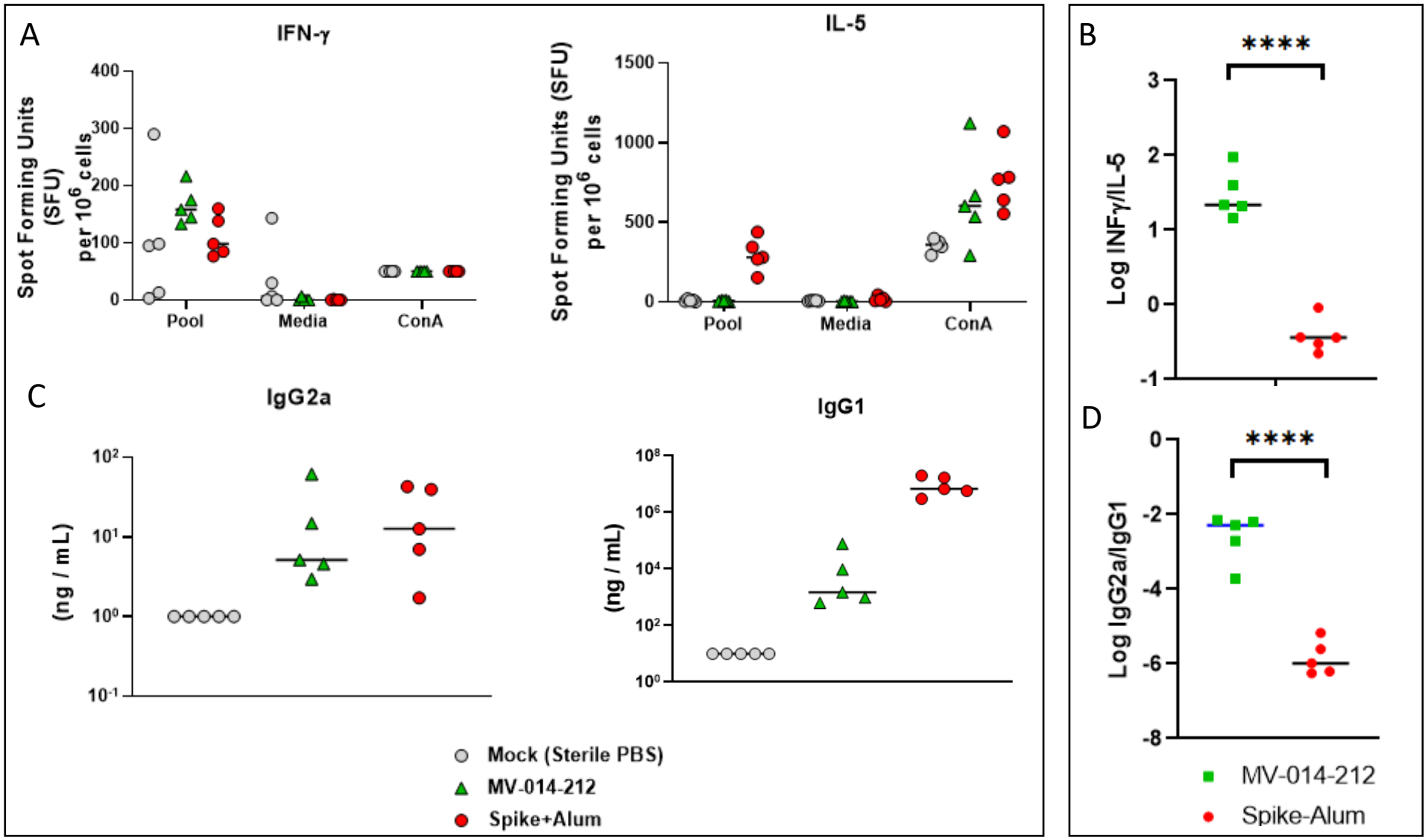
A
IFN-γ
Spot Forming Units (SFU) per 10^6 cells
400
300
200
100
0
Pool
Media
ConA
IL-5
Spot Forming Units (SFU) per 10^6 cells
1500
1000
500
0
Pool
Media
ConA
B
****
Log INFγ/IL-5
3
2
1
0
-1
C
IgG2a
(ng / mL)
10^2
10^1
10^0
10^-1
IgG1
(ng / mL)
10^8
10^6
10^4
10^2
10^0
D
****
Log IgG2a/IgG1
0
-2
-4
-6
-8
Mock (Sterile PBS)
MV-014-212
Spike+Alum
MV-014-212
Spike-Alum

Table 1 Intranasal COVID-19 vaccine in clinical development 2021

Platform	Description	Doses	Developer	Phase of clinical development
Live attenuated virus	Attenuated RSV expressing functional spike protein	1	Meissa	1
Live attenuated virus	COVI-VAC	1-2	Codagenix/Serum Institute of India	1
Replicating viral vector	DelNS1-2019-nCoV-RBD-OPT1 (Intranasal flu-based-RBD)	2	University of Hong Kong, Xiamen University and Beijing Wantai Biological Pharmacy	2
Non replicating viral vector	BBV154, Adenoviral vector COVID-19 vaccine	1	Bharat Biotech International Limited	1
Non replicating viral vector	ChAdOx1 nCOV-19	1-2	University of Oxford	1
Inactivated virus	Live recombinant Newcastle Disease Virus (rNDV) vector vaccine	2	Laboratorio Avi-Mex	1
Protein subunit	CIGB-669 (RBD+AgnHB)	3	Center for Genetic Engineering and Biotechnology (CIGB)	1/2